HelmholtzZentrum münchen
German Research Center for Environmental Health

Bayerisches NMR Zentrum

Technische Universität München

Structure, dynamics and molecular interactions of biological macromolecules by NMR

Winter School on Structural Cell Biology, CEITEC, Brno, Feb 9-13, 2015

Michael Sattler

http://www.nmr.ch.tum.de
http://www.helmholtz-muenchen.de/stb
http://www.bnmrz.org

Outline

Solution NMR methods to study protein complexes

- Ligand binding: CSP
- Optimized isotope labeling and NMR experiments
- Spin labeling: PRE (NMR), solvent PREs (sPRE)
- Large proteins, complexes, domain arrangements

Integrated structural biology of protein-RNA interactions

- Intron RNA recognition by multi-domain splicing factors (splicing regulation)
- [Cooperative mRNA recognition by Sxl/UNR (translational regulation)]

Structure/imaging from molecules to animals

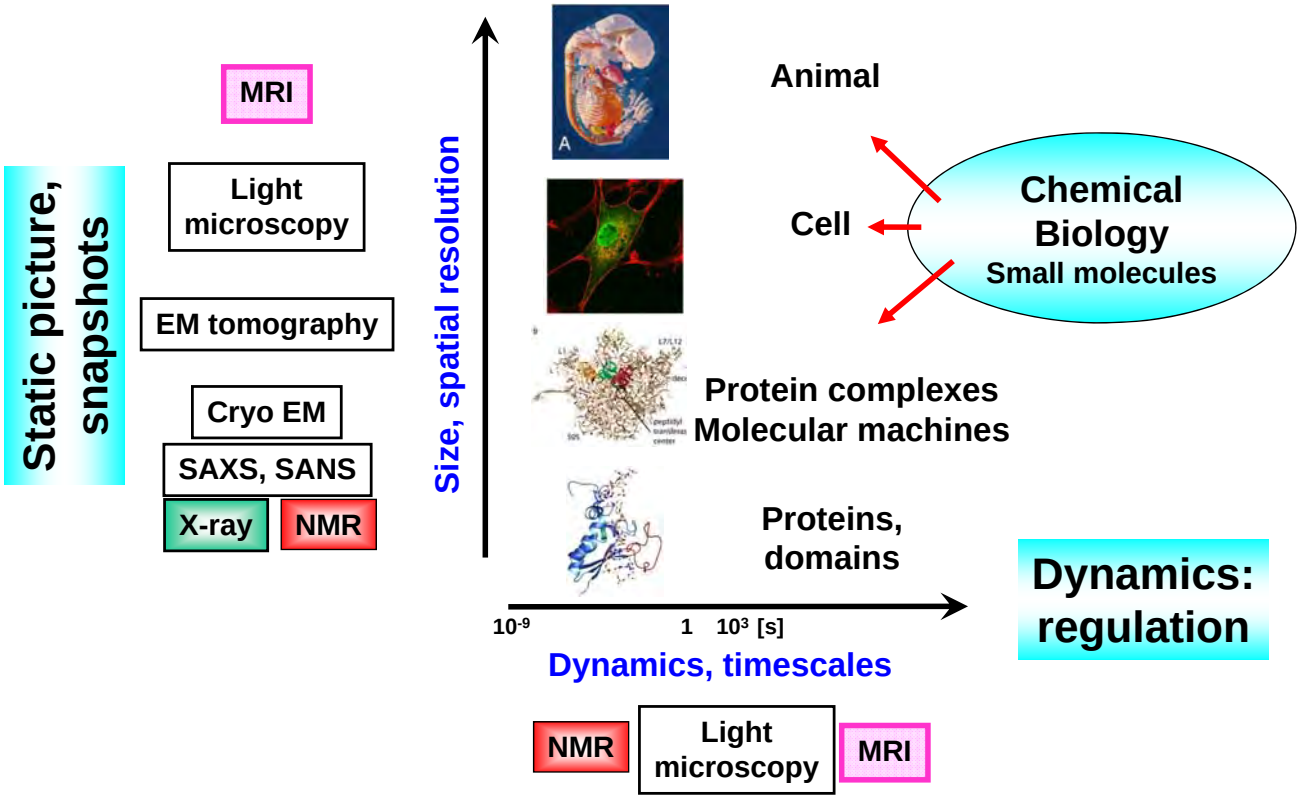

Why solution state NMR?

Nature 2007

LETTERS

Visualizing spatially correlated dynamics that directs RNA conformational transitions

Qi Zhang[1], Andrew C. Stelzer[1], Charles K. Fisher[1] & Hashim M. Al-Hashimi[1]

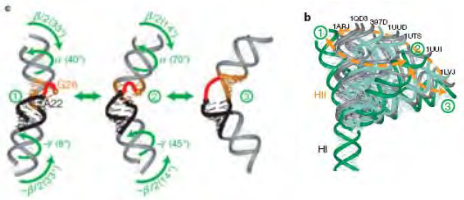

ARTICLES

Nature 2007

Intrinsic motions along an enzymatic reaction trajectory

Katherine A. Henzler-Wildman[1], Vu Thai[1], Ming Lei[1], Maria Ott[2], Magnus Wolf-Watz[1†], Tim Fenn[2†], Ed Pozharski[2†], Mark A. Wilson[2†], Gregory A. Petsko[2], Martin Karplus[2,3], Christian G. Hübner[3†] & Dorothee Kern[1]

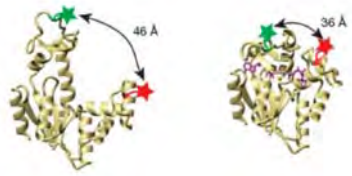

LETTER

Nature 2011

doi:10.1038/nature10171

Multi-domain conformational selection underlies pre-mRNA splicing regulation by U2AF

Cameron D. Mackereth[1,2,3], Tobias Madl[1,4], Sophie Bonnal[5], Bernd Simon[3], Katrá Zanier[4], Alexander Gasch[3], Vladimir Rybin[6], Juan Valcárcel[5,6] & Michael Sattler[1,3,4]

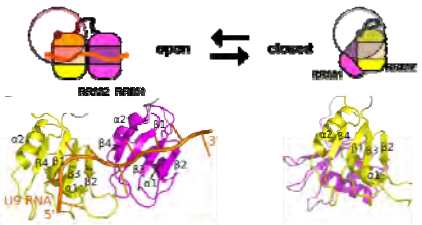

LETTERS

Nature 2009

High-resolution multi-dimensional NMR spectroscopy of proteins in human cells

Kohsuke Inomata[1,2], Ayako Ohno[1], Hidehito Tochio[1,2], Shin Isogai[1], Takeshi Tenno[2,4], Ikuhiko Nakase[5], Toshihide Takeuchi[5], Shiroh Futaki[5,3], Yutaka Ito[2,6], Hidekazu Hiroaki[2,4] & Masahiro Shirakawa[1,2,7]

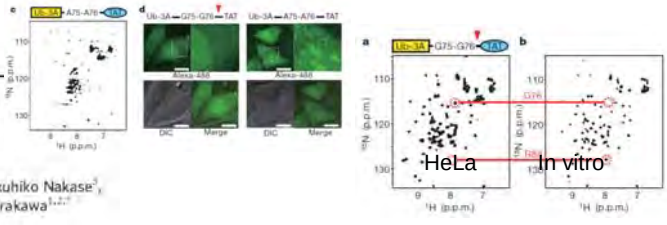

Biomolecular NMR

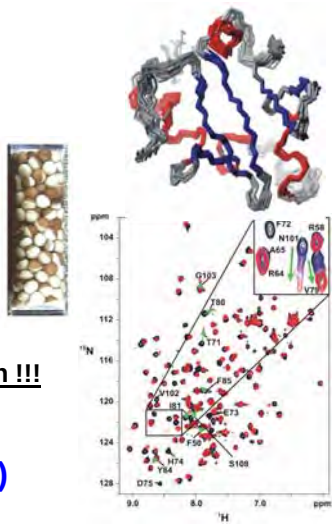

- **Structure determination of biomacromolecules**
  - → **no crystal needed, native-like conditions: solution, macromolecular crowding, *"in cell"* NMR (Xenopus oocytes)**
  - → **nucleic acids: difficult to crystallize, affected by crystal packing**

- **Ligand binding and molecular interactions in solution**
  - → **"Band shift" in NMR fingerprint - with residue/amino acid resolution !!!**

- **Characterization of dynamics and mobility (ps → days)**
  - → **conformational dynamics ↔ enzyme turnover, kinetics, folding**

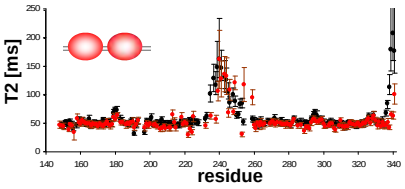

- **Molecular weight**: X-ray: >200 kDa,

  NMR: de novo structure <50 kDa, but: binding/dynamics: 900 kDa

- **→ NMR and X-ray crystallography are complementary**

Exp.Method	Proteins	Nucleic Acids	Protein/NA Complexes	Other	Total
X-RAY	59425	1276	2865	18	63584
NMR	7749	944	171	7	8871
ELECTRON MICROSCOPY	250	22	94	0	366
HYBRID	29	3	1	1	34
other	132	4	5	13	154
Total	67585	2249	3136	39	73009

www.pdbe.org

www.rcsb.org

Effect of exchange/dynamics on NMR spectra

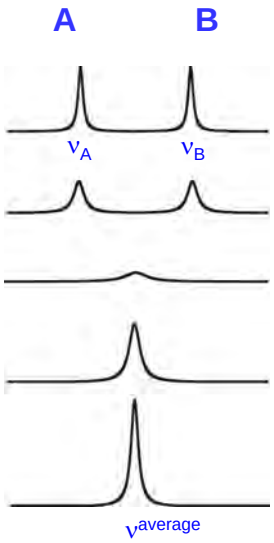

NMR time scale: chemical shift, i.e. resonance frequencies

slow exchange
$k_{ex} << \Delta\nu$

coalescence
$k_{ex} \sim \Delta\nu$

fast exchange
$k_{ex} >> \Delta\nu$

ν_A, ν_B: resonance frequency

$$A \underset{k_{-1}}{\overset{k_1}{\rightleftarrows}} B$$

$$k_{ex} = k_1 + k_{-1}$$

- Exchange process can be binding, conformational exchange, chemical reaction…
- Line widths and resonance frequencies depend on the exchange rates and frequency differences $\Delta\nu$ of the interconverting states
- Exchange can allow transfer of magnetization in 2D NOESY-type experiments
- Rate constants can be determined, for conformational or binding equilibrium, chemical reaction, ….

Göbl et al Sattler Prog NMR Spectrosc (2014)

Effect of dynamics on NMR spectra

$$A \underset{k_{-1}}{\overset{k_1}{\rightleftarrows}} B$$

$k_{ex} = k_1 + k_{-1}$

Population: 3:1

$\omega_A - \omega_B$ = 100 Hz

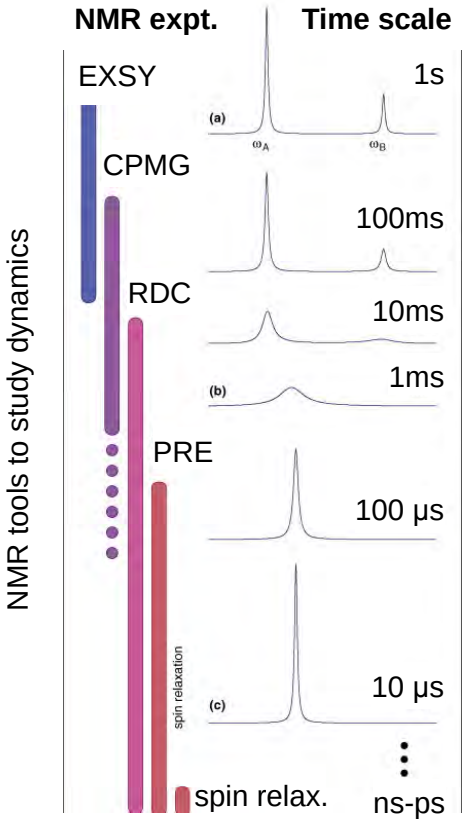

slow **exchange**
$k_{ex} \ll \Delta\nu$

coalescence
$k_{ex} \sim \Delta\nu$

fast **exchange**
$k_{ex} \gg \Delta\nu$

Mittermaier & Kay, TiBS 2009

Two-site exchange: protein/ligand interactions by NMR

slow exchange

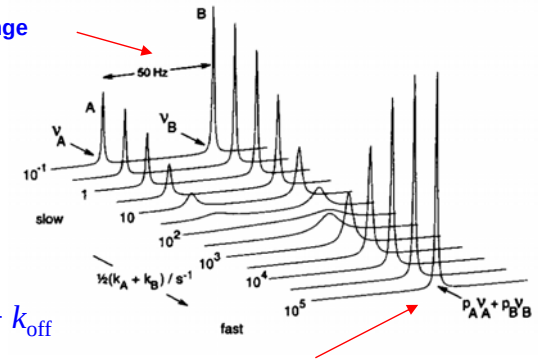

Fig. 4.7 Calculated NMR spectra for a pair of nuclei exchanging between two sites A and B with populations in the ratio $p_B/p_A = 2$ (unsymmetrical two-site exchange). Spectra are shown for a range of values of the average exchange rate $\frac{1}{2}(k_A + k_B)$, where $k_A/k_B = 2$. The difference in resonance frequencies of the two sites, $\delta\nu$, is 50 Hz. The linewidths in the absence of exchange are 1 Hz.

fast exchange

$k_{ex} = k_{on}[L] + k_{off}$

$$P + L \underset{k_{on}}{\overset{k_{off}}{\rightleftarrows}} PL$$

$K_D = [P][L] / [PL] = k_B/k_A$

$k_A = k_{on}[L]$; $k_B = k_{off}$

B = protein-ligand complex PL

A = free protein P

This can be used to determine, e.g. residue pK_a values or **dissociation constants K_d**.

Limit	Rates	Populations	Line broadening
Slow	$k_{A,B} \ll (\nu_A - \nu_B)$	$p_A/p_B = \text{area}_A/\text{area}_B$	$\Delta\nu_A = k_A/\pi = 1/(\pi\,\tau_A)$
Fast	$k_{A,B} \gg (\nu_A - \nu_B)$	$p_A = (\nu - \nu_B)/(\nu_A - \nu_B)$	$\Delta\nu = 4\pi p_A p_B\,(\nu_A - \nu_B)^2/(k_A + k_B)$

Ligand binding in NMR titrations (fast exchange)

K_D > [P] (µM-mM) ➔ K_D can be fitted

Binding in <u>fast</u> exchange on the NMR chemical shift time scale

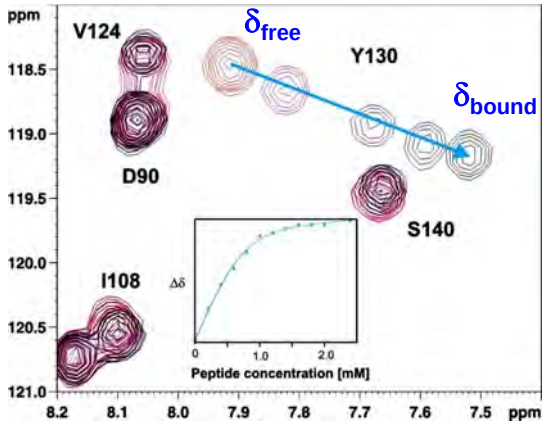

Binding of a RG-rich peptide to SMN Tudor domain

***equilibrium dissociation constant* K_D**
from binding isotherm

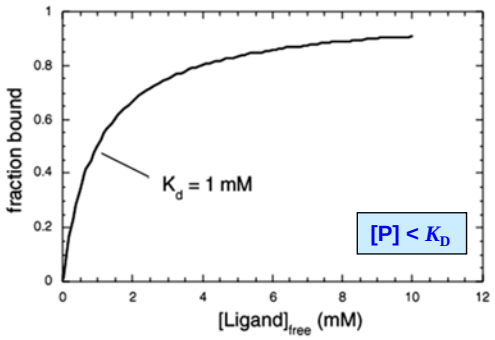

$$P + L \underset{k_{off}}{\overset{k_{on}}{\rightleftarrows}} PL$$

Fraction bound

$[PL] \sim \Delta\delta = \delta_{obs} - \delta_{free} = f([L_{tot}])$

$K_D = [P][L] / [PL] = k_B/k_A$

$k_A = k_{on}[L]$; $k_B = k_{off}$

B = protein-ligand complex PL

A = free protein P

Viral B2 protein dimer: inhibitor of RNAi

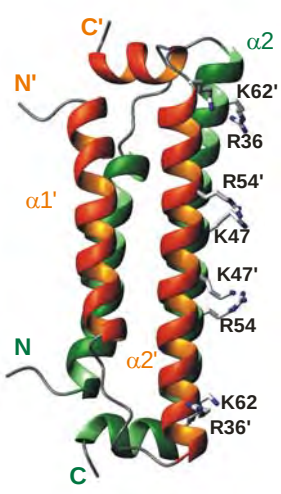

B2 dimer

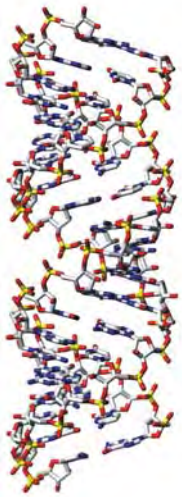

19 bp dsRNA

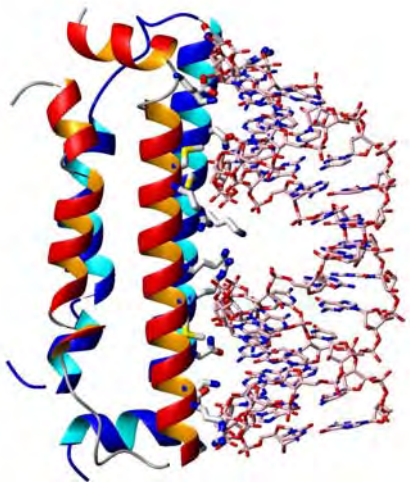

Lingel et al (2005) *EMBO reports*

Chao et al, Williamson (2005) *NSMB*

Ligand binding in NMR titrations (slow exchange)

K_d < [P] (nM) ➔ binding stoichiometry can be determined

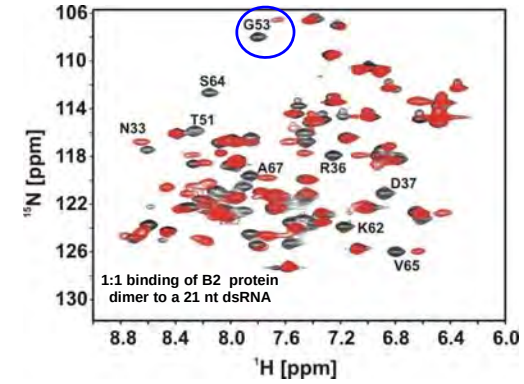

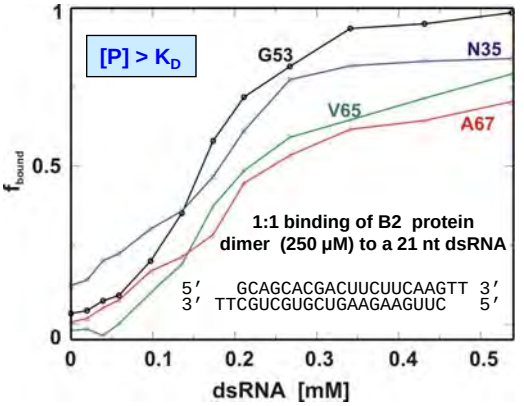

Binding stoichiometry
(from inflection point of titration curve)

Binding in <u>slow</u> exchange
on the NMR chemical shift time scale

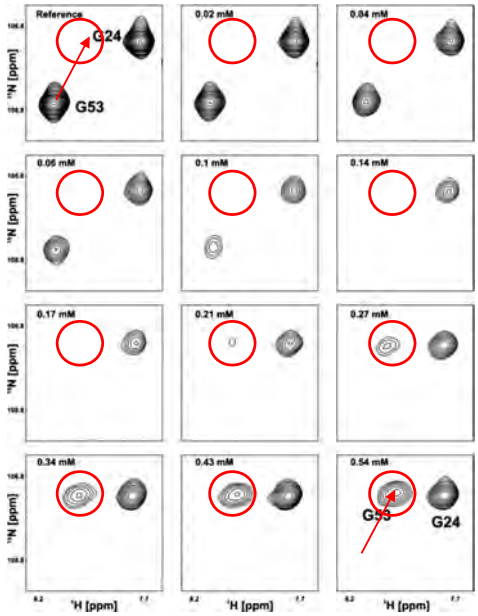

Ligand binding - stoichiometry

- Stoichiometry can only be correct if protein concentration is accurately determined!

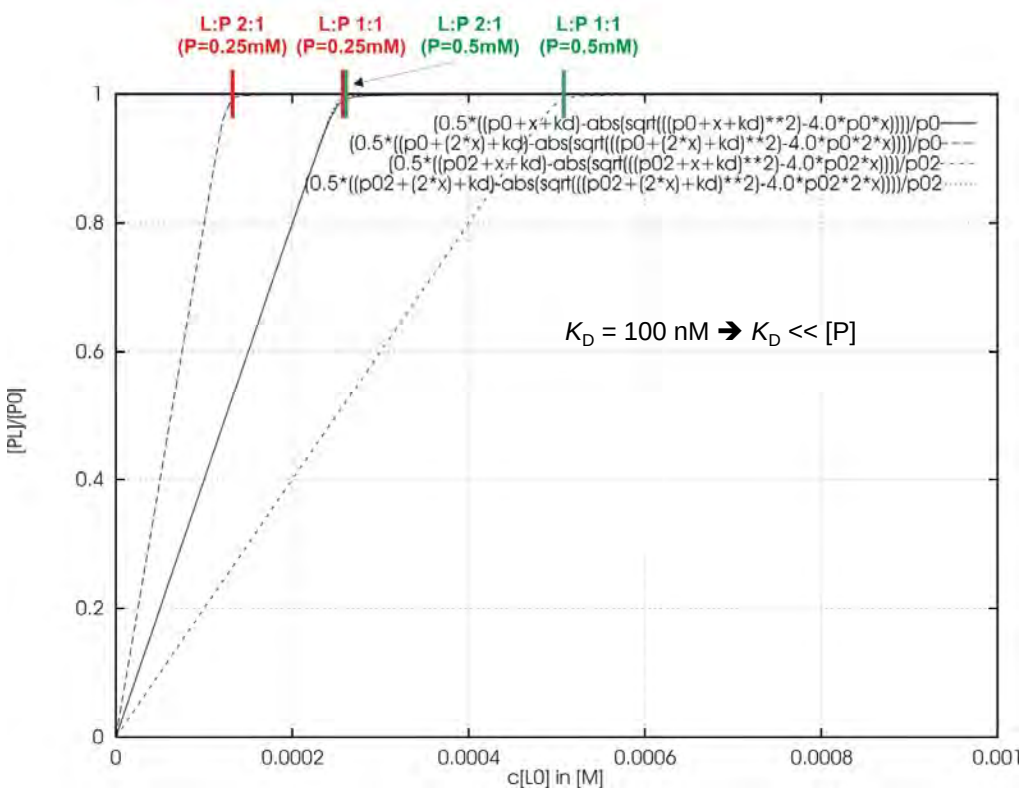

NMR titrations – large complexes

Binding of a small ligand to a large protein:

Bound state may be broadened beyond detection.

$$I(\omega) = \mathrm{re}\int_0^\infty W \exp\{i(\Omega - \omega E)t + Kt + Rt\}\,1\,dt \quad (1)$$

Line shape simulation of a system in slow exchange with a bound state having a large molecular weight.
The fraction of free protein is 0.5. R_f=23 s^{-1};R_b=250 s^{-1}; k_{off} = 25 s^{-1}
Chemical shift differences Δδ = 0 (black) and 500 Hz (red).
The resonance position of the free state, ω_1=250 Hz.

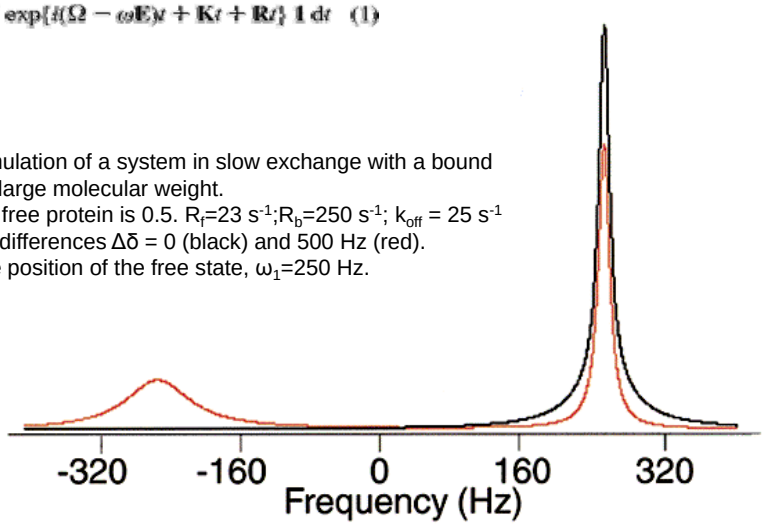

Identification by NMR Spectroscopy of Residues at Contact Surfaces in Large, Slowly Exchanging Macromolecular Complexes.
Matsuo, et al & Wagner (1999) JACS 121, 9903-4.

Kinetics and thermodynamics from NMR line shape analysis

- k_{ex} is obtained from measuring transverse relaxation / linewidth fitting
- Temperature dependence allows to determine activation enthalpy and entropy based on Arrhenius/Eyring transition state theory

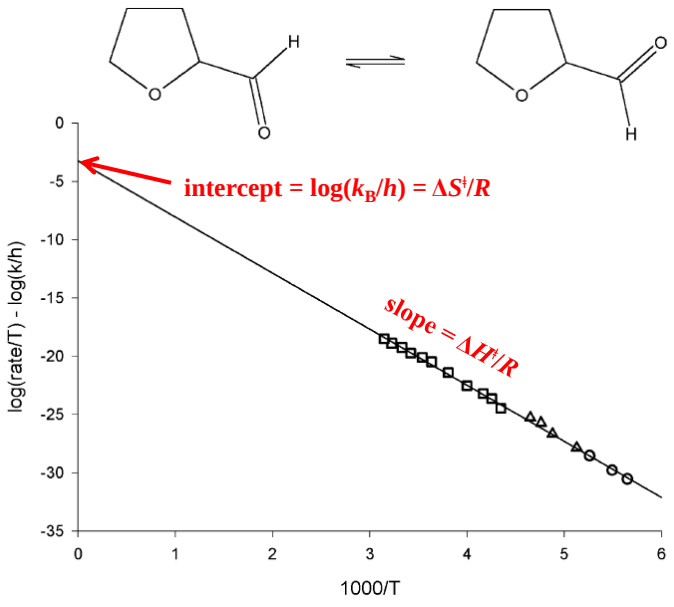

Eyring equation

$$k = \frac{k_B T}{h}\exp(-\Delta G^{\dagger}/RT)$$

$$= \frac{k_B T}{h}\exp(\Delta S^{\dagger}/R - \Delta H^{\dagger}/RT)$$

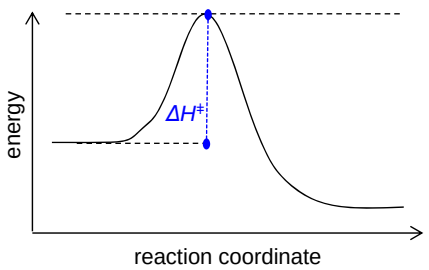

Bain A.D. *Prog NMR Spectroscopy* (2003) 43, 63-103.; Kessler H. *Angew Chem* (1970) 9, 219-235.

Exchange spectroscopy (EXSY)

$$d\boldsymbol{M}_z(t) = -(\boldsymbol{R}+\boldsymbol{K})\,\boldsymbol{M}_z(t)$$

$$A \underset{k_{BA}}{\overset{k_{AB}}{\rightleftarrows}} B$$

$$k_{ex} = k_{AB} + k_{BA}$$

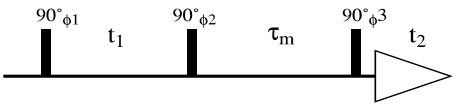

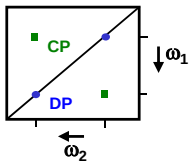

$$\boldsymbol{R} = \begin{pmatrix} \frac{1}{T_1} & 0 \\ 0 & \frac{1}{T_1} \end{pmatrix} \qquad \boldsymbol{K} = \begin{pmatrix} k_{AB} & -k_{BA} \\ -k_{AB} & k_{BA} \end{pmatrix}$$

$$\begin{pmatrix} M_{A,z}(t) \\ M_{B,z}(t) \end{pmatrix} = e^{-[\boldsymbol{R}+\boldsymbol{K}]t} \begin{pmatrix} M_{A,z}(0) \\ M_{B,z}(0) \end{pmatrix}$$

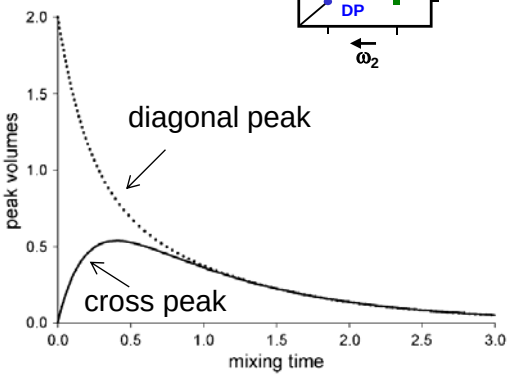

For symmetric 2-site exchange:

$k_{AB} = k_{BA};\quad k_{ex} = k_{AB} + k_{BA}$

equal population: $p_A = p_B$

$$a_{II}(t) = a_{SS}(t) = \tfrac{1}{2} \exp\{-\rho t\}\,[1 + \exp(-2k_{ex}t)]$$
$$a_{IS}(t) = a_{SI}(t) = \tfrac{1}{2} \exp\{-\rho t\}\,[1 - \exp(-2k_{ex}t)]$$

$\rho = R_1 = 1/T_1$

$k_{ex} = k_{AB} + k_{BA}$

Exchange spectroscopy

Cyclophilin A - proline cis/trans isomerase, HIV capsid protein

O diagonal peak

O cross peak

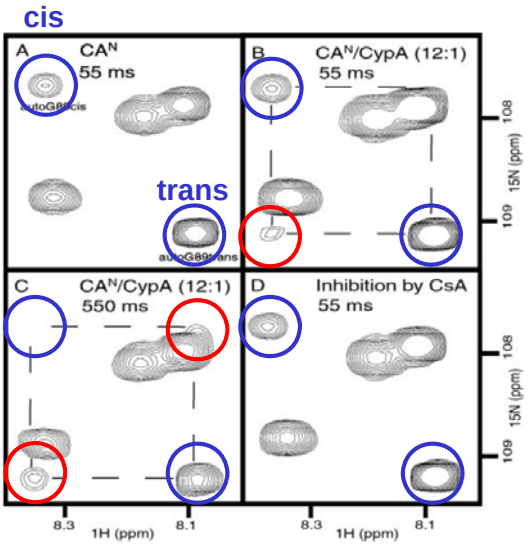

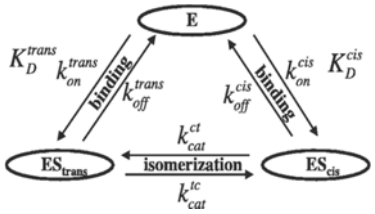

Kern et al, PNAS 2002

NMR of large protein complexes: ClpP

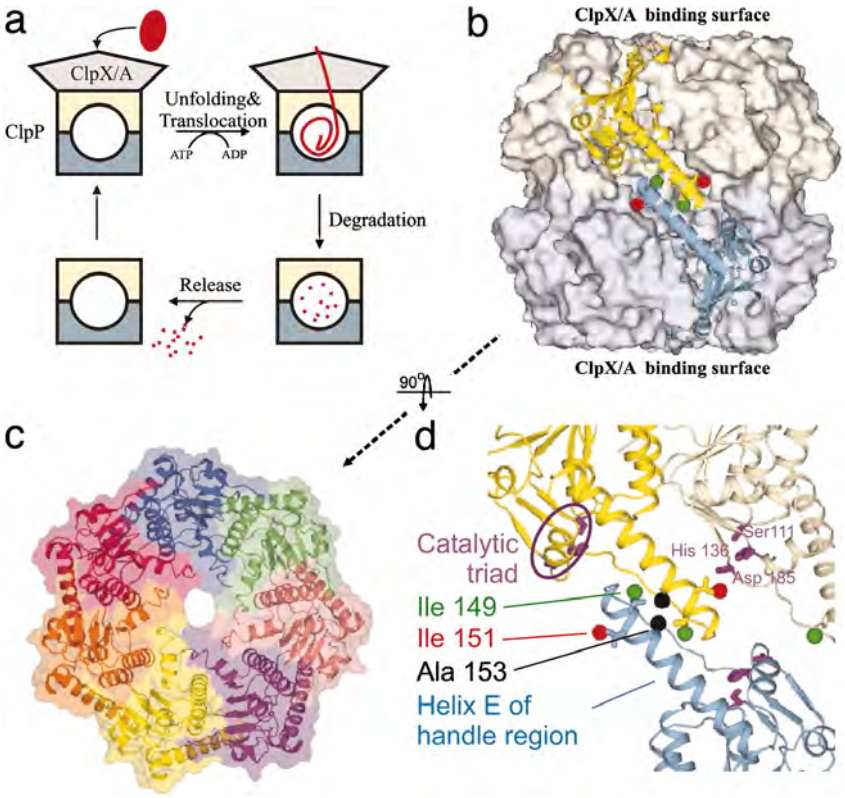

Sprangers R et al. Kay LE PNAS 2005;102:16678-16683

Conformational exchange in ClpP

^{1}H, ^{13}C methyl TROSY NMR
of U-[^{15}N,^{2}H], Ile δ_1-[^{13}C,^{1}H] ClpP

Two NMR signals disappear upon mutation of a single Ile
- Ile δ_1 sees 2 different conformational states
- Confirmed by temperature dependence

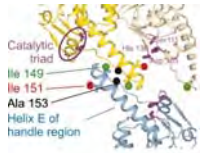

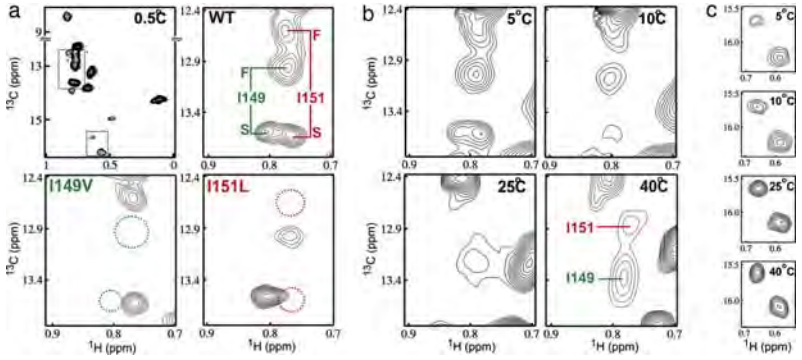

Exchange spectroscopy to quantitate the F,S exchange process

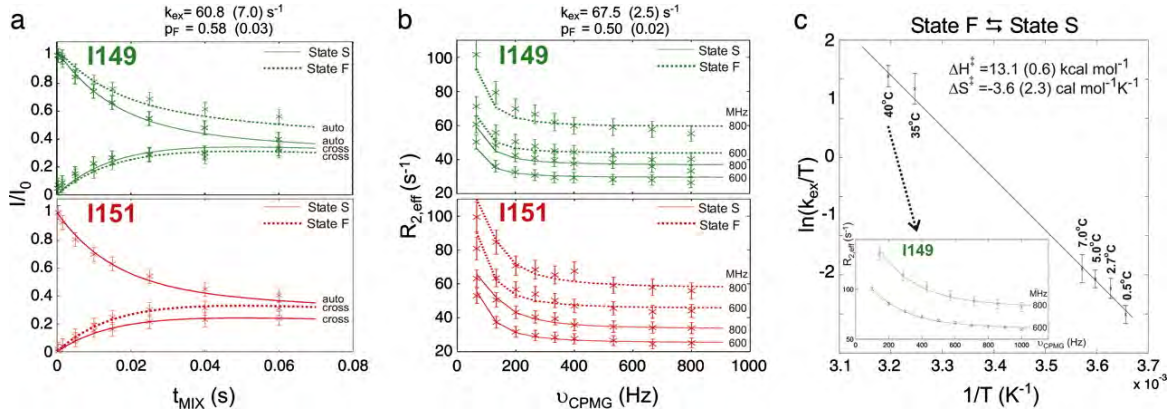

Sprangers R et al. Kay LE PNAS 2005;102:16678-16683

Ligand detected NMR screening: Saturation Transfer Difference (STD)

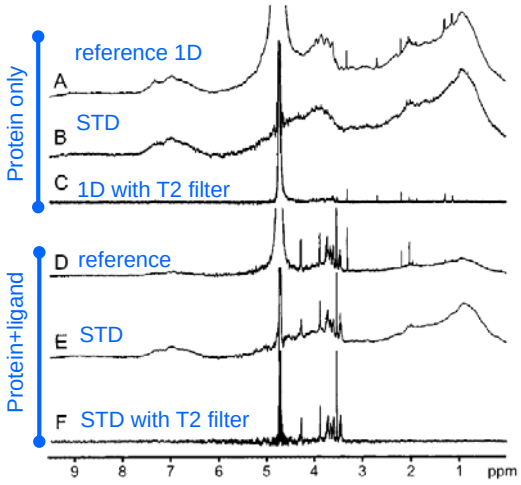

Figure 1. (A) Reference 1D NMR spectrum of the 120-kDa lectin RCA_{120} (50 μM in binding sites), displaying the very broad lines normal for a protein this size. The few sharp resonances arise from low-molecular-weight impurities. (B) Corresponding STD NMR spectrum showing that, by irradiating at −2 ppm, the entire protein is saturated uniformly and can therefore be efficiently used for the STD NMR technique. One can also see that the impurities contained in the spectrum are effectively subtracted and therefore do not give rise to signals in the difference spectrum. (C) 1D NMR spectrum recorded with a $T_{1\rho}$ filter, consisting of a 30-ms spin-lock pulse, to eliminate the broad resonances of the protein. Only those resonances of the low-molecular-weight impurities remain in the spectrum. (D) Reference 1D NMR spectrum of RCA_{120} (40 μM in binding sites) in the presence of 1.2 mM β-GalOMe, without the $T_{1\rho}$ filter. (E) Corresponding STD NMR spectrum showing that β-GalOMe yields signals and therefore binds to the receptor. (F) STD NMR spectrum as in (E) but with the $T_{1\rho}$ filter eliminating all protein background signals.

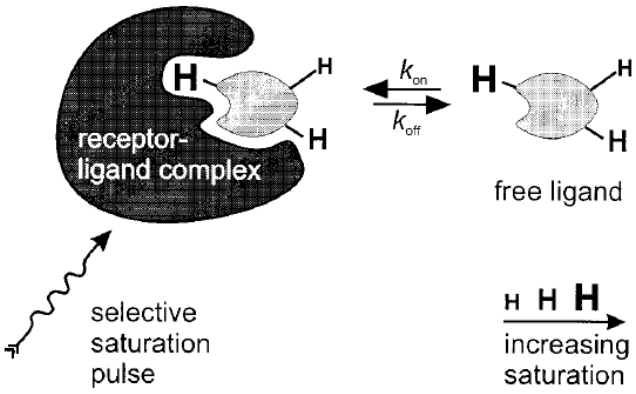

- Saturation Transfer Difference (STD) NMR
- WATER-LOGSY, T2, diffusion filters, …

- Little amount of target protein needed
- No size limitation for target protein
- Provides binding epitope mapping → SAR
- Detect micromolar binders (K_D 10^{-3}-10^{-8}) or competition for nanomolar ligands

B Meyer et al , Angew Chem 1999; JACS 2001

NOE and ROE

NOESY

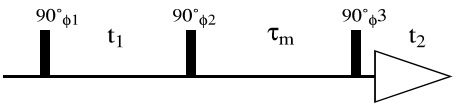

ROESY

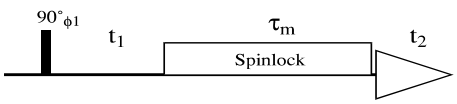

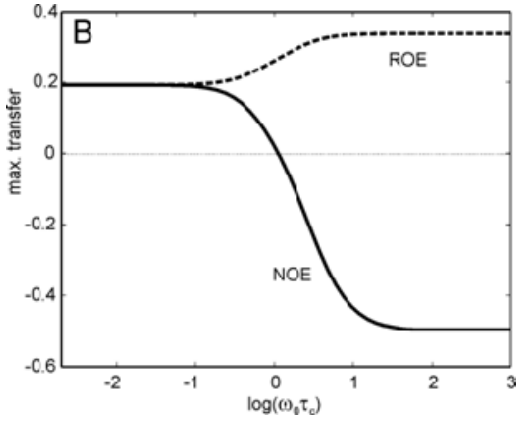

Extreme narrowing limit
Positive NOE
$W_2 > W_0$

Slow tumbling limit
Negative NOE
$W_2 << W_0$

2D NOESY spectra of a small ligand free and bound to a protein

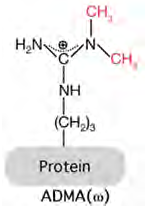

Free ligand (aDMA)

Negative NOE cross peaks,
Positive diagonal peaks

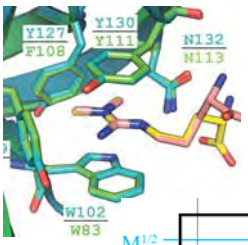

Protein-ligand complex*
(aDMA/SMN Tudor)

Positive NOE cross peaks
Positive diagonal peaks

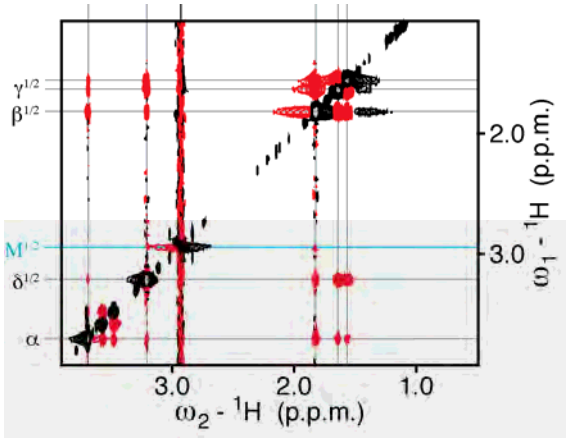

1mM ADMA

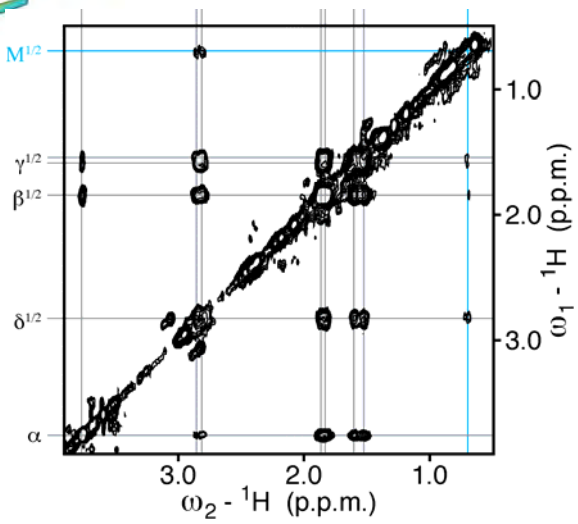

*with large excess of protein to observe mainly bound ligand

1mM ADMA, 4mM SMN Tudor

Tripsianes et al, Nature Struct Mol Biol (2011)

Isotope edited/filtered experiments

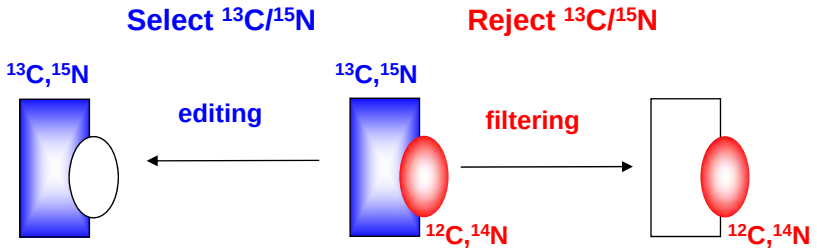

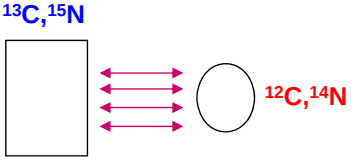

edited/filtered
NOESY experiments

Principle combinations of editing/filtering

Editing/filtering can be applied before t_1 and/or t_2 → ω_1 and/or ω_2-edited/filtered correlations

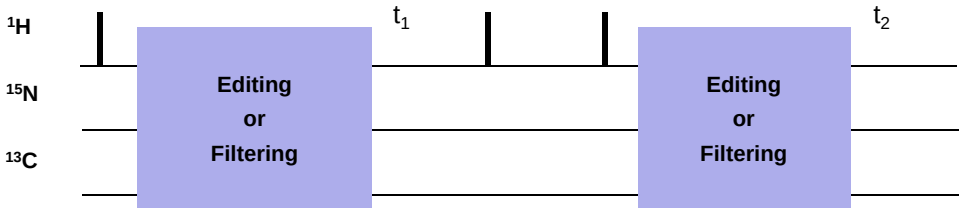

ω_2 filtered NOESY

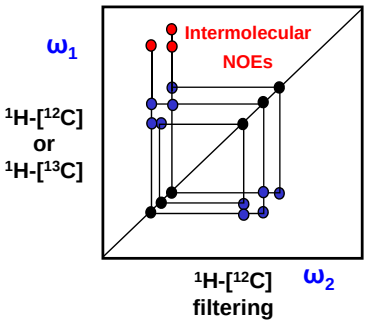

ω_1-edited, ω_2-filtered NOESY

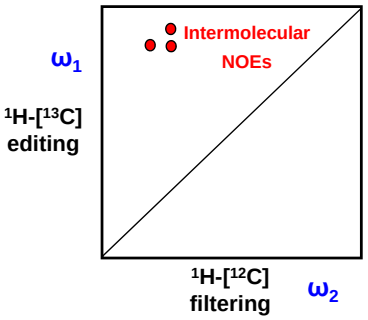

Isotope filtered 2D NOESY

Triple ^{13}C filter (2x $^{13}C^{aliphatic}$, $^{13}C^{aromatic}$) , single ^{15}N filter

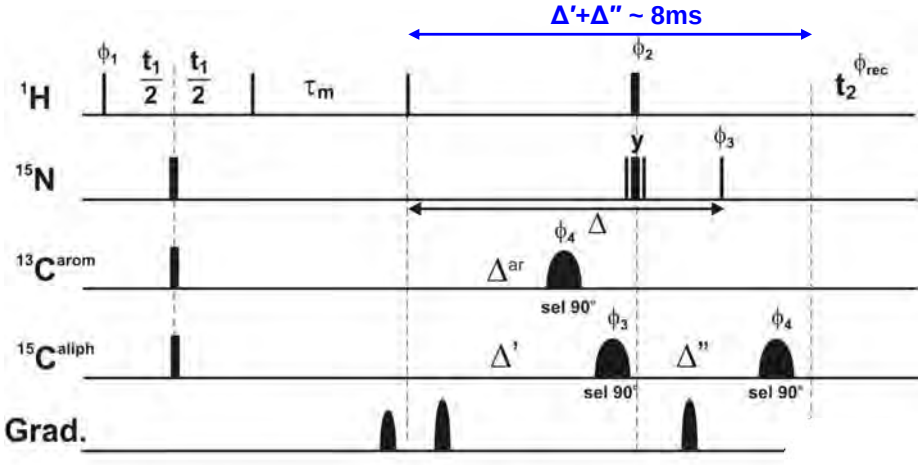

Δ=5.4ms; Δ'=3.5ms; Δ''=4.0ms;τ_p(sel. 90°)=400 µs;
ϕ_1= x, -x; ϕ_2= 2(x),2(y); ϕ_3= 4(x), 4(-x); ϕ_4= 8(y), 8(-y); ϕ_{rec}= x, -x, -x, x.

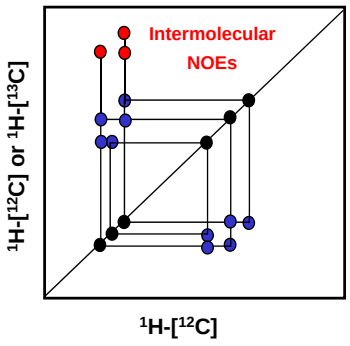

1D (protein + RNA)

1D filter experiment (RNA only)

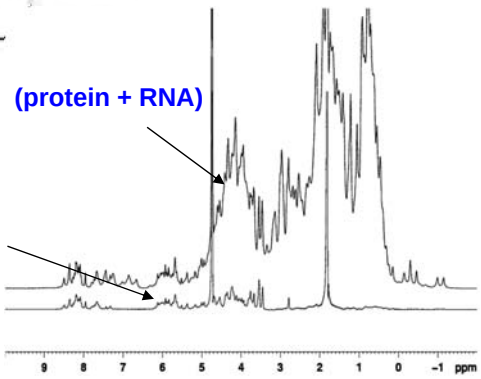

Sattler, Schleucher, Griesinger, Prog NMR Spectrosc (1999)

3D edited/filtered NOESY of protein-RNA complex

$^{1}H \rightarrow {}^{13}C\ (t_1) \rightarrow {}^{1}H(-{}^{13}C)\ (t_2) \rightarrow$ NOE $\rightarrow$ filter $\rightarrow {}^{1}H(-{}^{12}C/{}^{14}N)\ (t_3)$

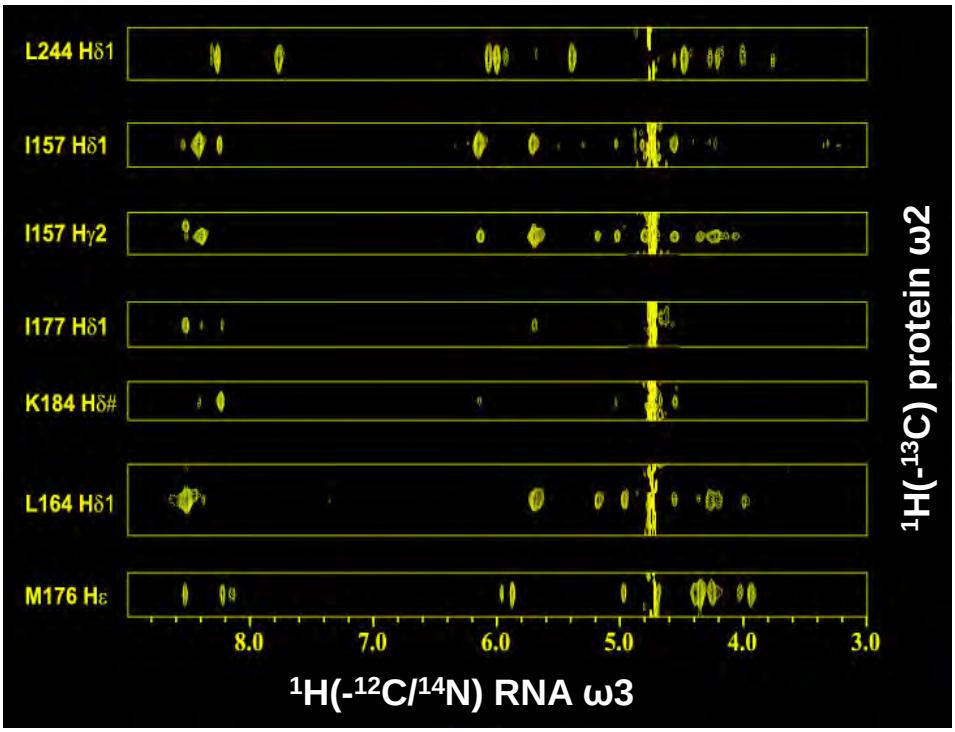

3’ splice site recognition in constitutive splicing

- Essential early step in pre-mRNA splicing
- Regulation of alternative splicing during **spliceosome assembly**
- **Cooperative recognition** of 3’ splice site by U2AF and SF1

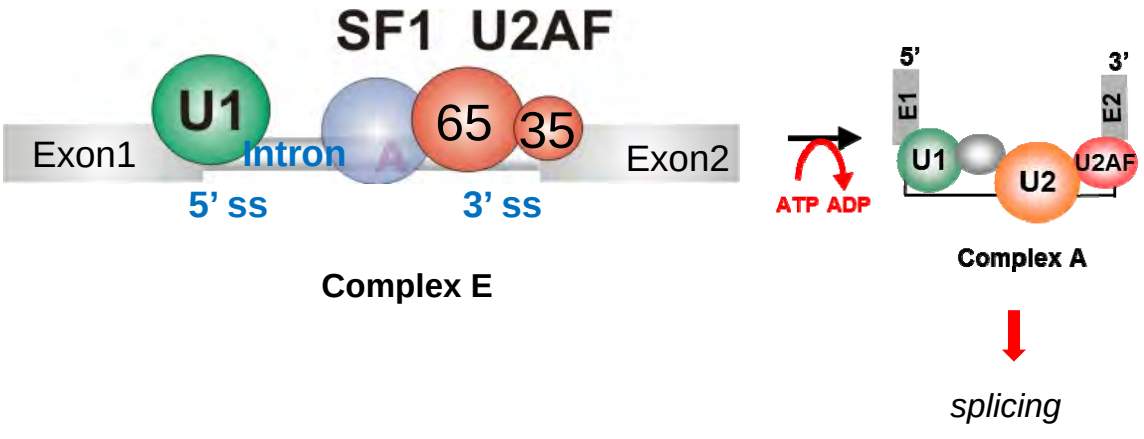

Structural modules at the 3’ splice site

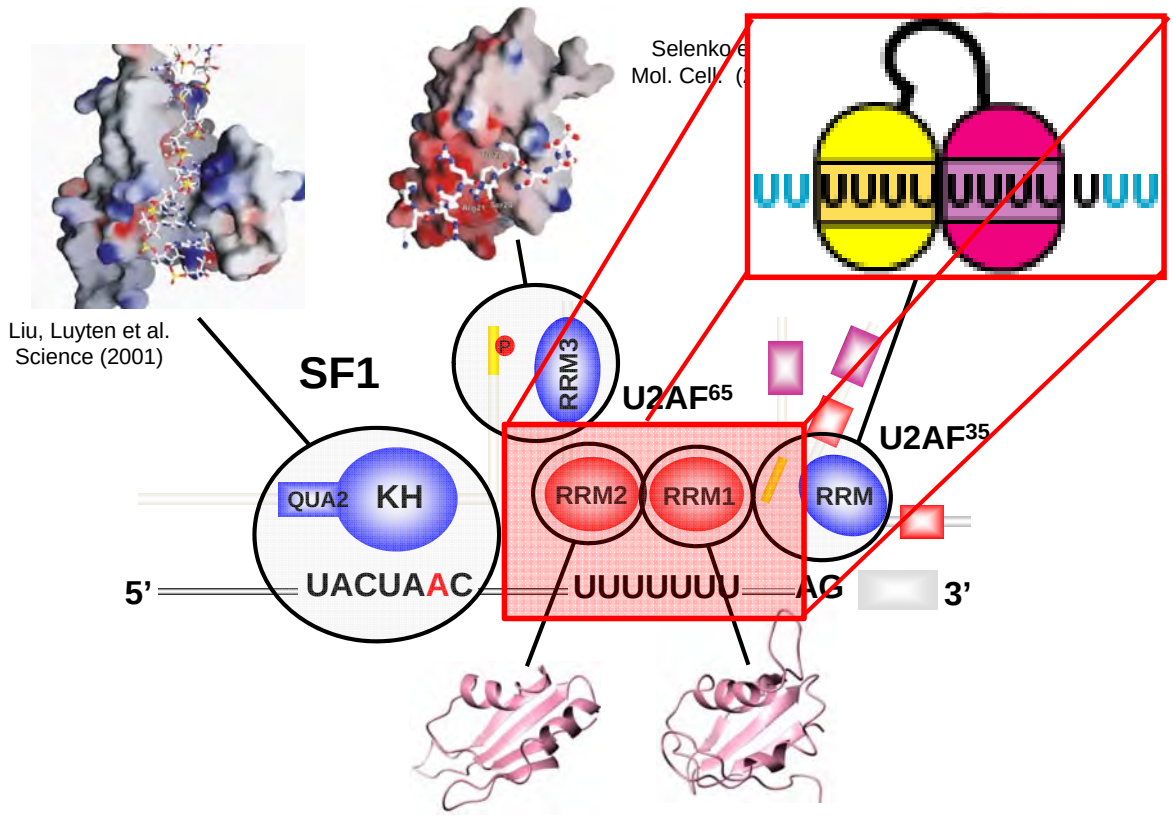

Ito et al. EMBO J. (1999); Sickmier et al Mol.Cell (2006); Mackereth et al Sattler Nature (2011) *i*

Dynamics in multi-domain protein interactions

Multi-domain dynamics

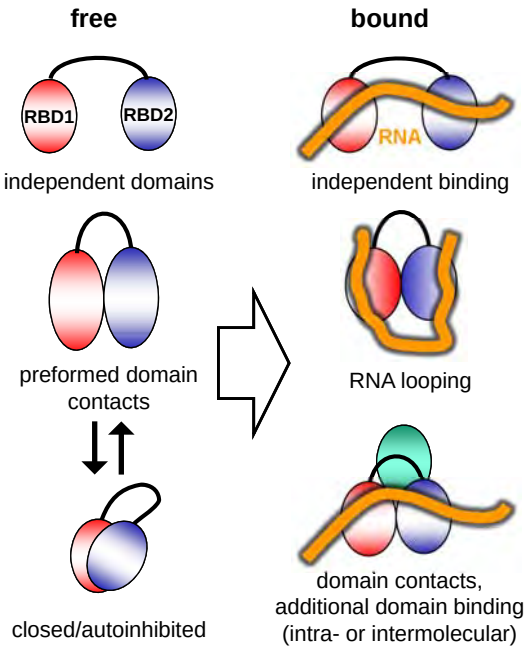

Multiple register binding

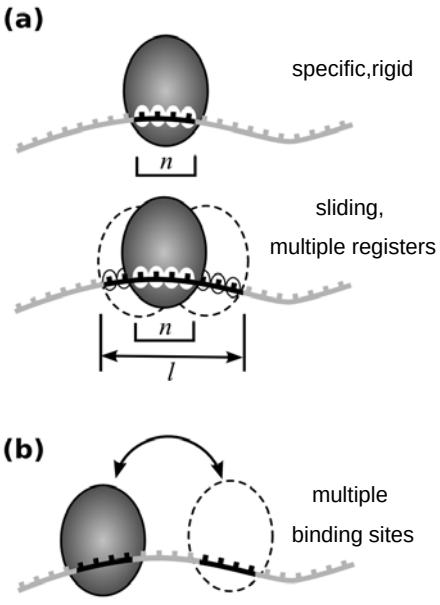

Mackereth & Sattler, Curr Op Struc Biol 2012

NMR approaches for studying large complexes

- **3D structure of subunits available (X-ray, NMR, ROSSETTA)**
- **Subunit-selective/segmental labeling**
  Sortase A ligation, optimized ^{2}H-labeling
  → sensitivity, spectral simplification

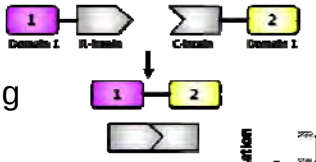

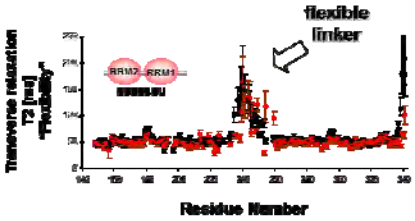

- **Conformational dynamics: NMR relaxation**
- **Domain interfaces/intramolecular contacts**
  Chemical shift perturbations (CSP)
  PREs (spin labeling): ~ $1/r^6$, <20Å
  Solvent PREs

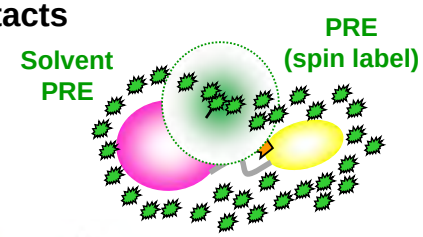

- **Domain arrangements**
  Residual dipolar couplings (RDCs)
  Small angle scattering (SAS)
- **Structure calculations**
  Joint refinement NMR data / scoring with SAXS/SANS

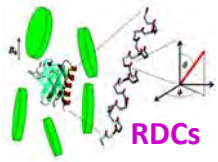

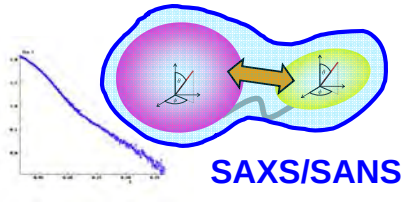

Simon, et al Angew. Chem (2010) ; Madl et al JACS (2010) ; Madl et al Angew. Chem (2011);
Madl et al J Struct Biol (2011); Hennig & Sattler Protein Sci (2014); Göbl et al Prog NMR Spec (2014)

Py tract RNA recognition by U2AF65 RRM1-RRM2

- U2AF is an essential splicing factor, required for intron Py tract RNA recognition
- U2AF65 RRM1-RRM2 necessary and sufficient for Py tract RNA binding
- Two structural domains, connected by a flexible linker

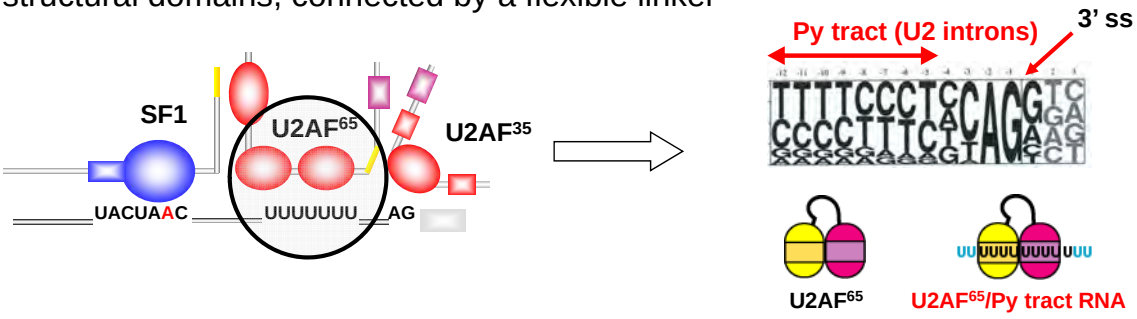

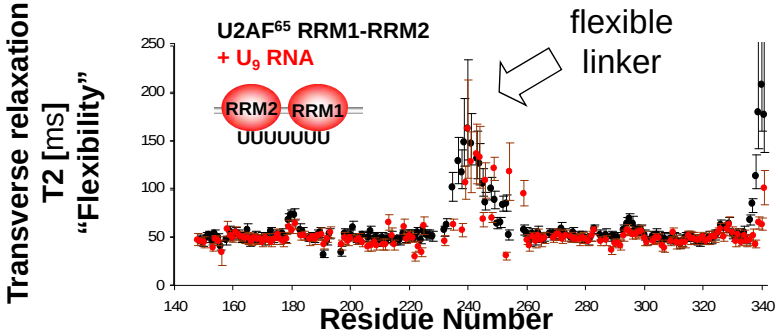

Subunit-selective labeling

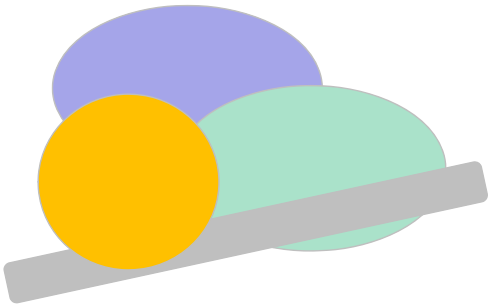

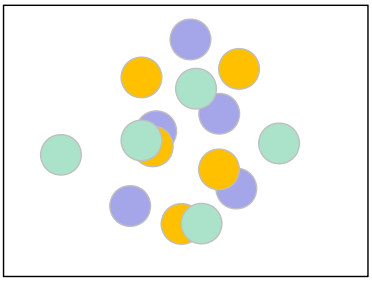

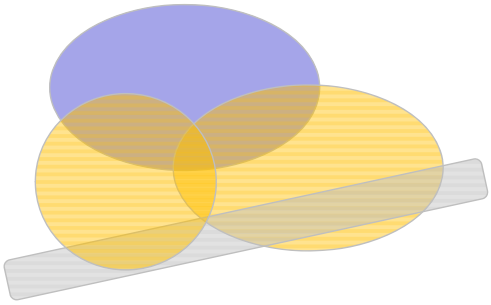

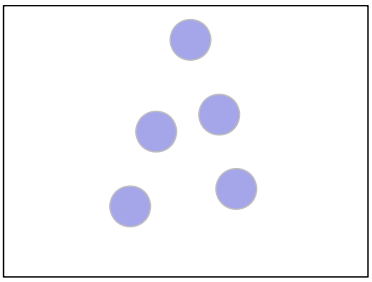

Utility of ^{2}H-labeling: SF1/U2AF/RNA (74 kDa)

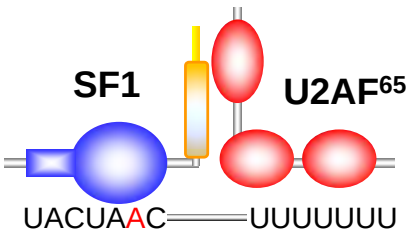

TROSY 600 MHz, 0.2 mM, 16 hours

[50%-2H,15N] U2AF65 + SF1 + RNA (74 kDa)

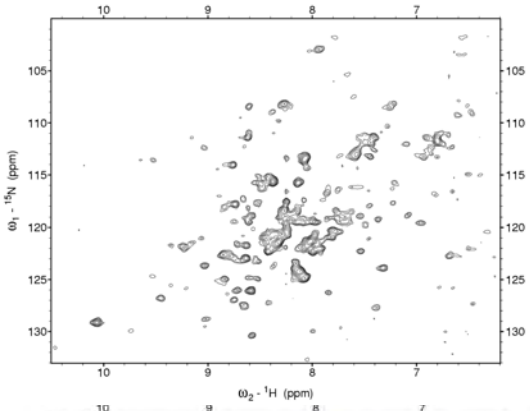

TROSY 600 MHz, 0.2 mM, 2 hours

[U-2H,15N] U2AF65 + SF1 + RNA (74 kDa)

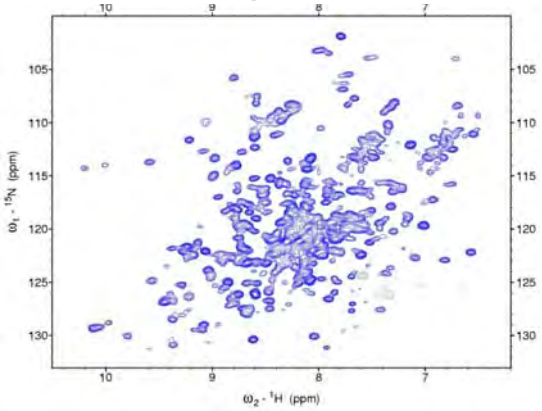

Random fractional deuteration and methyl-selective $^{1}H,^{13}C$ labeling

Random fractional ^{2}H-labeling

- Grow bacteria in 70-90% D_2O
  ➔ random fractional (60-80%) ^{2}H-labeling
- Cost-effective
- But: presence of $^{13}CH_x$ isotopomers
  ➔ combine with CH multiplicity filters

Sibille et al (2002) *JACS* 124 14616-25
Gardner & Kay (1998) *Ann Rev Biophys Biomol Struct* 27 357-406

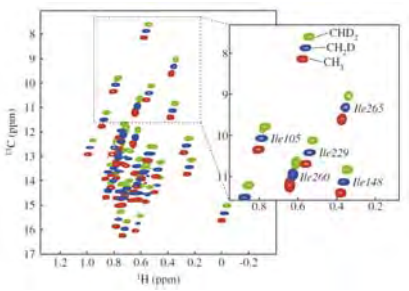

Ollerenshaw, et al Kay JBNMR 2005

ILV labeling: methyl-$^{13}C,^{1}H$ for Ile, Leu, Val

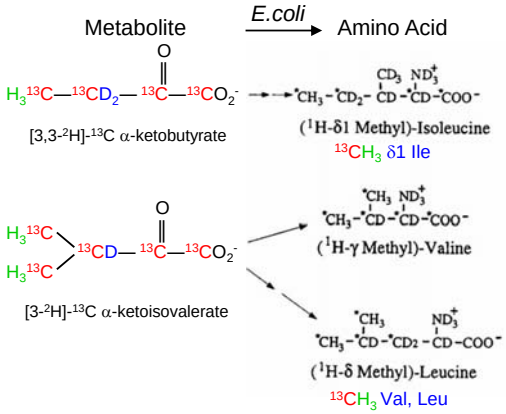

Gardner & Kay (1997) JACS 119 7599
Goto et al. (1999) *J. Biomol. NMR* 13 369-374

Residual dipolar couplings (RDCs)

In anisotropic solution:

- D!=0 ⇔ orientation
- Weak (10^{-4}) alignment in dilute (3-5%) liquid crystalline medium

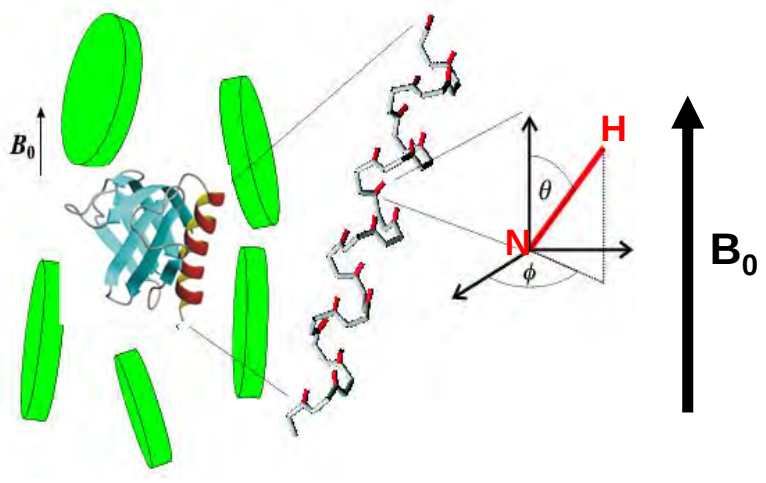

$D_{ij} \sim 1/r_{ij}^3 \langle(3\cos^2\theta-1)\rangle$
!= 0 in anisotropic solution

Residual dipolar coupling

Domain orientation from RDC data

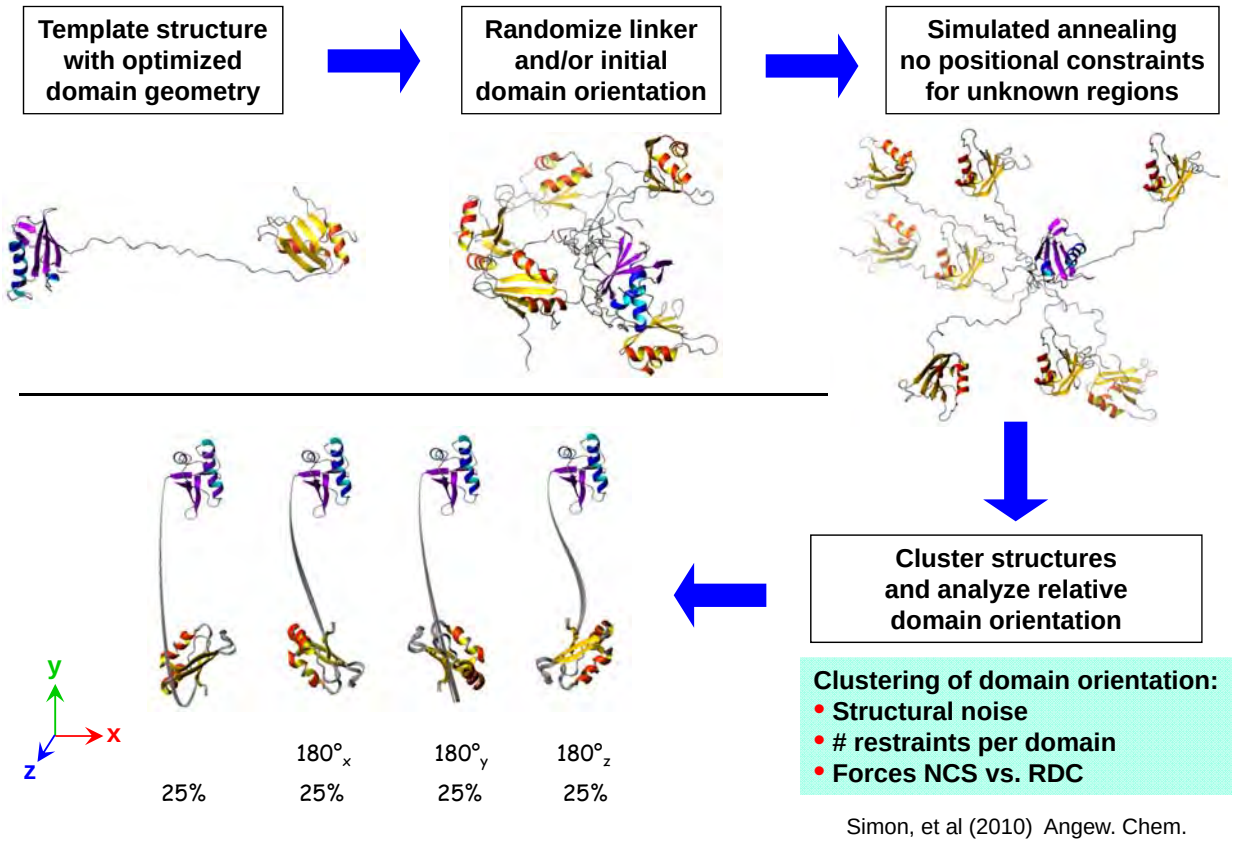

Clustering of domain orientation:
- **Structural noise**
- **# restraints per domain**
- **Forces NCS vs. RDC**

Simon, et al (2010) Angew. Chem.

Domain orientation with two alignment tensors

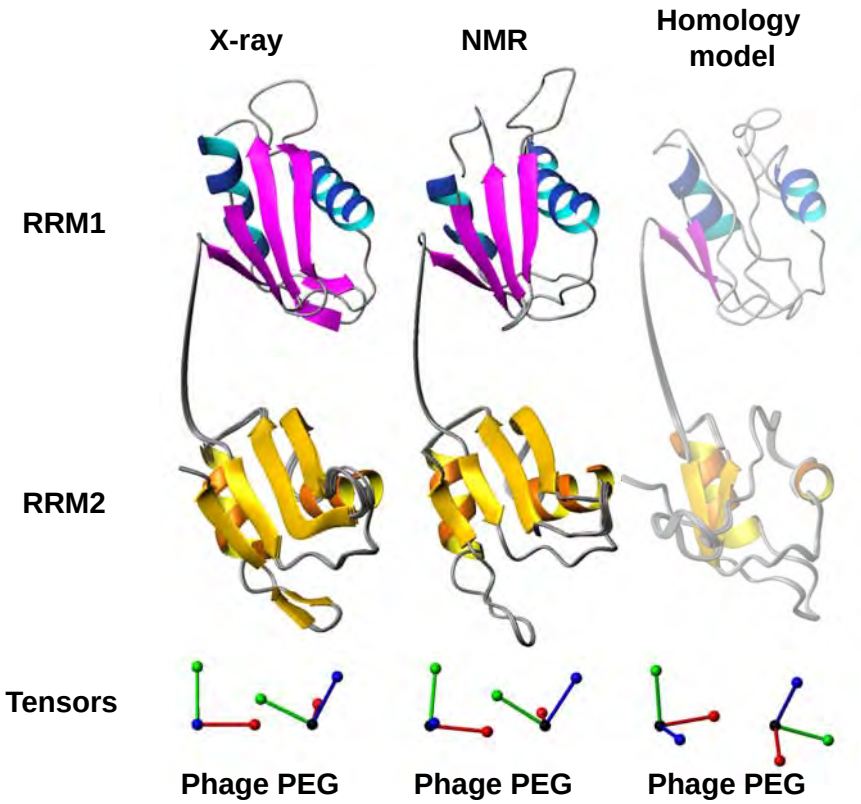

Important factors for domain orientation:
- **Structural noise (input)**
- **# RDCs per domain**
- **Coupling to reference**

Simon, et al (2010) Angew. Chem.

NMR restraints from paramagnetic effects

How to make your protein paramagnetic:

Metal-binding proteins

- **Paramagnetic metals binding sites**
- **PRE, PCS, RDC**

Paramagnetic tags (spin labels)

- **nitroxide radicals**
- **lanthanide-binding peptide tags**
  - **protein fusions with LBTs**
  - **covalently linked to cysteines,**
- **4-thio-uracyl, 2' amino (RNA)**
- **PRE, PCS, RDC**

Soluble paramagnetic agents

- **nitroxide radicals, ions, chelates**
- **Solvent PRE**

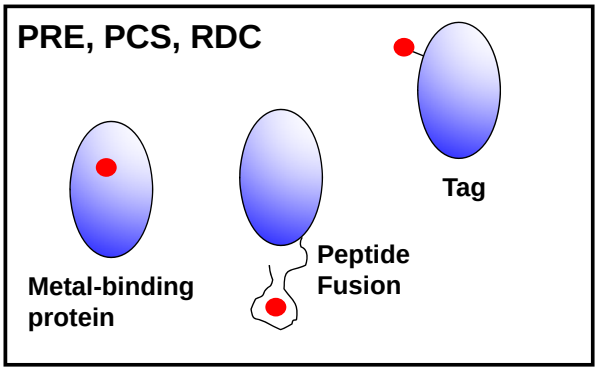

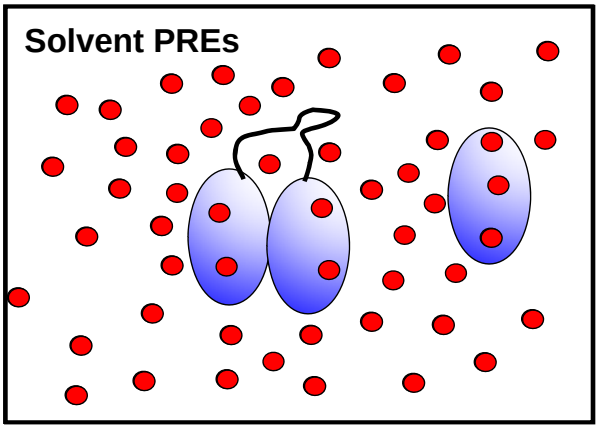

Madl. et al Angew Chemie (2009, 2011); Otting JBNMR 2008
Göbl et al Prog NMR Spec (2014)

Spin labeling of proteins and nucleic acids

Protein spin labeling:

Recombinant protein with single Cys mutant proteins
→ site-directed mutagenesis

MTSL often used (EPR, NMR)
IPSL chemically more stable,
but also less reactive

MTSL

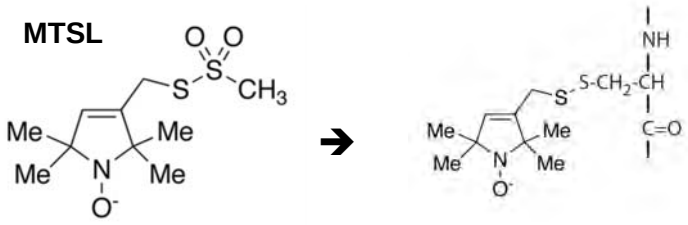

IPSL 3-[2-iodoacetamido]-proxyl

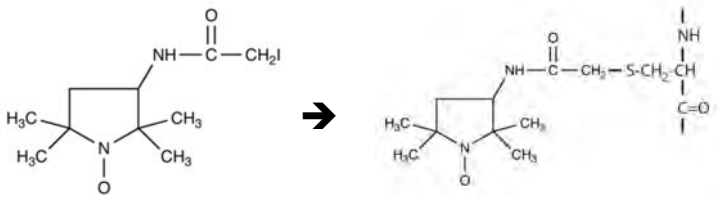

RNA spin labeling:

Chemically synthesize thiouracil RNA oligo

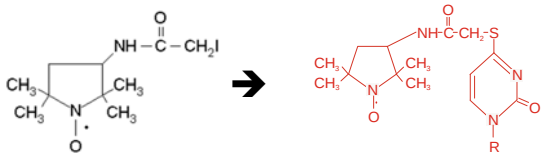

IPSL
3-[2-iodoacetamido]-proxyl

4-thiouracil proxyl
Varani JACS (1998)

Interdomain distance restraints from PREs

(paramagnetic relaxation enhancement)

- **PRE ~ r^{-6} (electron-spin distance)**
- → long-range distance restraints (<20 Å)
- → multiple single-Cys mutants of protein (→ molecular biology)
- Measure transverse PRE R_2^{PRE} from sample with oxidized (I_{para}) and reduced (I_{dia}) spin label

$$R_2^{PRE} = \frac{1}{15} S(S+1)\gamma_H^2 g^2 \mu_B^2 \frac{1}{r^6} \left(4\tau_c + \frac{3\tau_c}{1+\omega_H^2 \tau_c^2} \right)$$

Spin labeling **IPSL** 3-[2-iodoacetamido]-proxyl

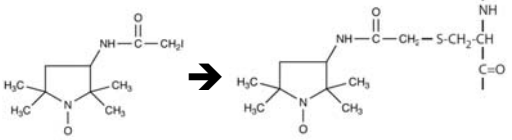

Measuring distances between domains

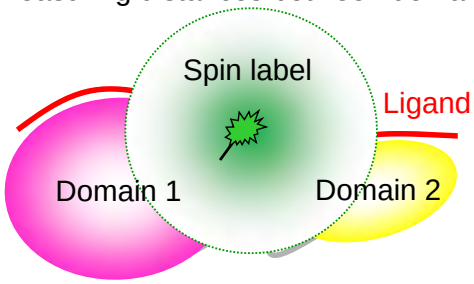

Reference expt (I_{dia}) Paramagnetic (I_{para})

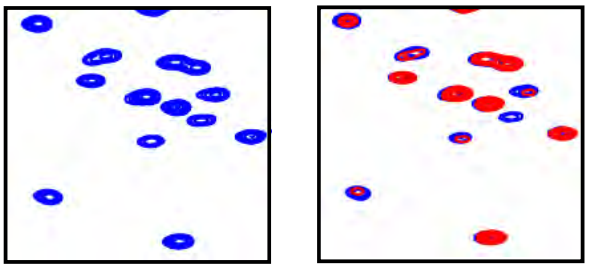

$$\frac{I_{para}}{I_{dia}} = R_2^{dia} \frac{\exp\left(-R_2^{PRE}\tau\right)}{R_2^{dia} + R_2^{PRE}}$$

Battiste & Wagner Biochemistry (2000); Simon, et al Angew. Chem. (2010); Madl et al J Struct Biol (2011)

Measuring $^1H^N$ PRE as Γ_2 directly

- 2-point measurement of exponential decays
- accurate, systematic errors ($^3J_{HN,Ha}$) cancel

$$\Gamma_2 = R_{2,para} - R_{2,dia} = \frac{1}{T_b - T_a} \ln \frac{I_{dia}(T_b) I_{para}(T_a)}{I_{dia}(T_a) I_{para}(T_b)}$$

- Set T_a=0,
- T_b=1.15/($R_{2,dia}$+Γ_2) to minimize error in Γ_2

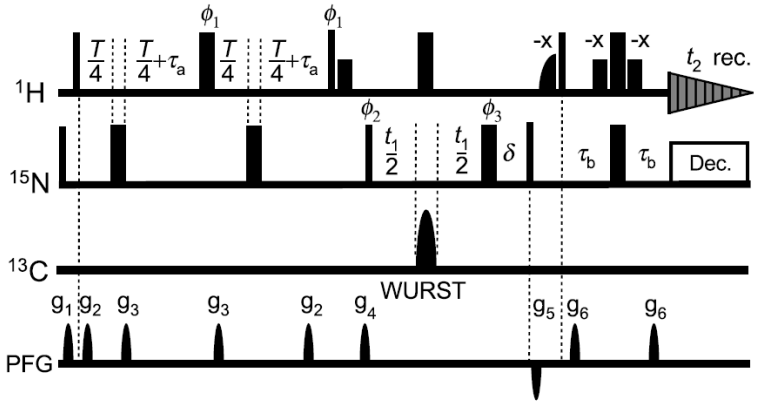

Fig. 1. Pulse sequence for ^1H_N-Γ_2 measurements. The delay T is changed for the relaxation measurement. Thin and bold bars indicate rectangular 90° and 180° pulses, respectively. Phases are along x unless indicated otherwise. Short bold bars represent soft rectangular 90° pulses (1.4 ms) selective for the ^1H_2O resonance. A half-bell shape for ^1H represents a half-Gaussian 90° pulse selective for water (2.0 ms). Delays are as follows: τ_a = 2.7 ms; τ_b = 2.25 ms; δ = (length of ^{13}C WURST pulse). Phase cycling: ϕ_1=(y,y,$-y$,$-y$); ϕ_2 = (x,$-x$); ϕ_3= (x,x,$-x$,$-x$,y,y,$-y$,$-y$); receiver=(x,$-x$,$-x$,x,$-x$,x,x,$-x$). The receiver phase and ϕ_2 were incremented for states-TPPI quadrature detection in the t_1 domain. Field gradients are optimized to minimize the solvent signal. Although $^3J_{HN\text{-}H\alpha}$ is active for non-deuterated proteins during the period T, the resulting modulation is cancelled out when Γ_2 is calculated as described in the main text.

Donaldson et al Kay, J.Am.Chem.Soc. (2001)123, 9843–9847. Iwahara et al.Clore J Mag Res (2007) 184,185–195

PRE in the presence of exchange/dynamics

Fast exchange allows detection of minor species

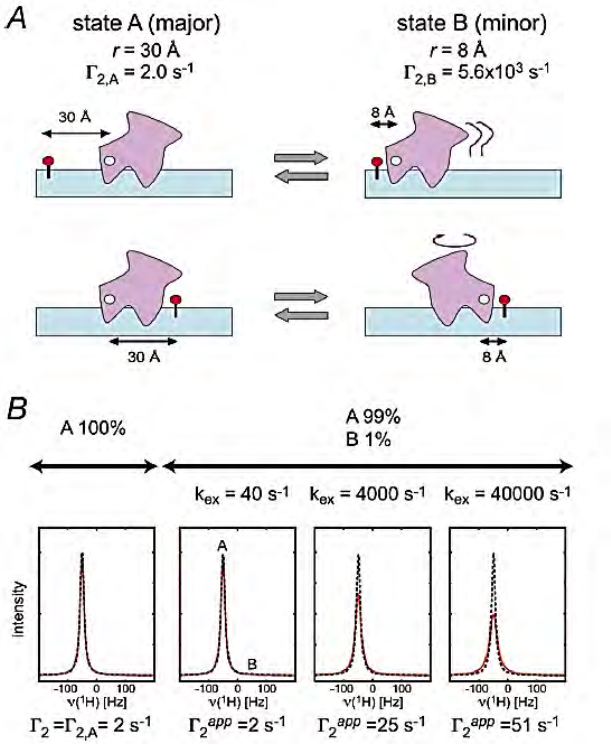

Assume: $k_{ex} \gg |\Gamma_{2,B} - \Gamma_{2,A}|$

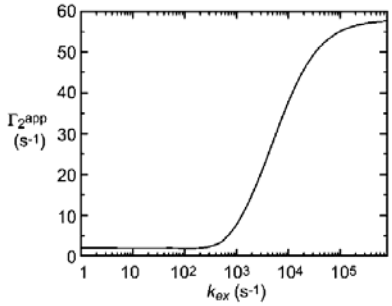

Otherwise, if: $|\Omega_A - \Omega_B| \ll k_{ex} \ll |\Gamma_{2,B} - \Gamma_{2,A}|$

need to now $\Delta\Omega$ and k_{ex}

PRE may become independent of *r*

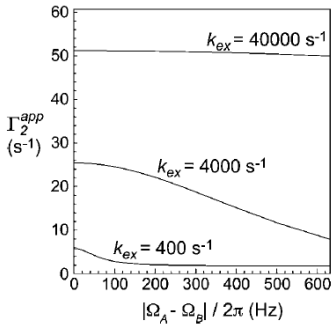

Clore & Iwahara, Chem Rev (2009)

Paramagnetic Relaxation Enhancement (PRE)

- **Distance calibration:** linear approximation for $0.2 < I^{ox}/I^{red} < 0.8$
- **Estimate τ_c** from $(R_2/R_1)^{ox}$ and $(R_2/R_1)^{red}$

  Note: τ_c refers to the electron-nuclear spin vector!
- **Grid search for correlation time τ_c for each SL**

$$R_2^{PRE} = \frac{1}{15} S(S+1)\gamma_H^2 g^2 \mu_B^2 \frac{1}{r^6}\left(4\tau_c + \frac{3\tau_c}{1+\omega_H^2\tau_c^2}\right)$$

$$r = 370\text{Å} * \sqrt[6]{\frac{1}{R_2^{PRE}}\left(4\tau_c + \frac{3\tau_c}{1+\omega_H^2\tau_c^2}\right)}$$

$$\frac{I_{para}}{I_{dia}} = R_2^{dia}\,\frac{\exp\left(-R_2^{PRE}\tau\right)}{R_2^{dia}+R_2^{PRE}}$$

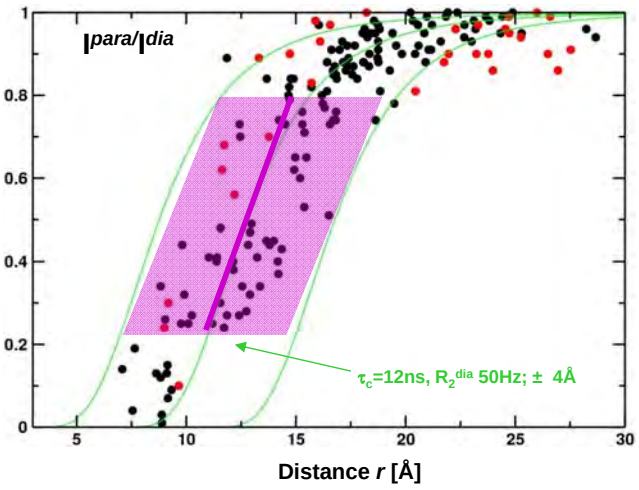

Experimental vs. calculated distance

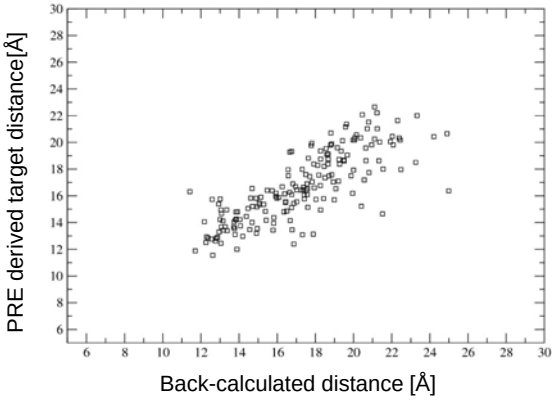

Battiste & Wagner *Biochemistry* (2000), Simon et al Angew Chem (2010)

Spin label flexibility and τ_c of the electron - H_N vector

Flexibility of the spin label

- Consider internal flexibility and conformational space sampled by the spin label by a ensemble representation (i.e. 4 copies per spin label site)
- ensemble averaged distance restraints during structure calculations

$$\langle r^{-6} \rangle = \frac{1}{N n_p} \sum_{h}^{N} \sum_{s}^{n_p} r_{hs}^{-6}$$

Iwahara, Schwieters, Clore JACS (2004) 126,5879-5896

Estimation of the electron-spin correlation time τ_c

- Need to determine/estimate τ_c from $(R_2/R_1)^{ox}$ and $(R_2/R_1)^{red}$
- Grid search for correlation time τ_c for each SL

$$Q = \sqrt{\frac{\sum_i \{\Gamma_2^{obs}(i) - \Gamma_2^{cal}(i)\}^2}{\sum_i \Gamma_2^{obs}(i)^2}}$$

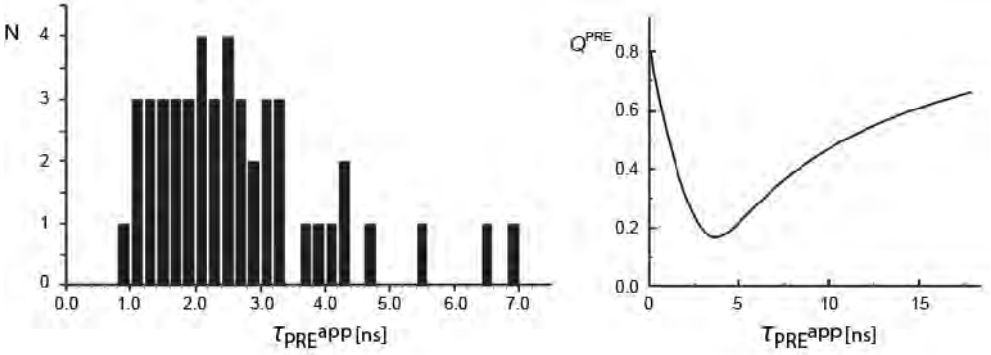

Simon, et al Angew. Chem. (2010); Hennig et al, Sattler Methods Enzym (2015)

Structure calculation from RDC + PRE data

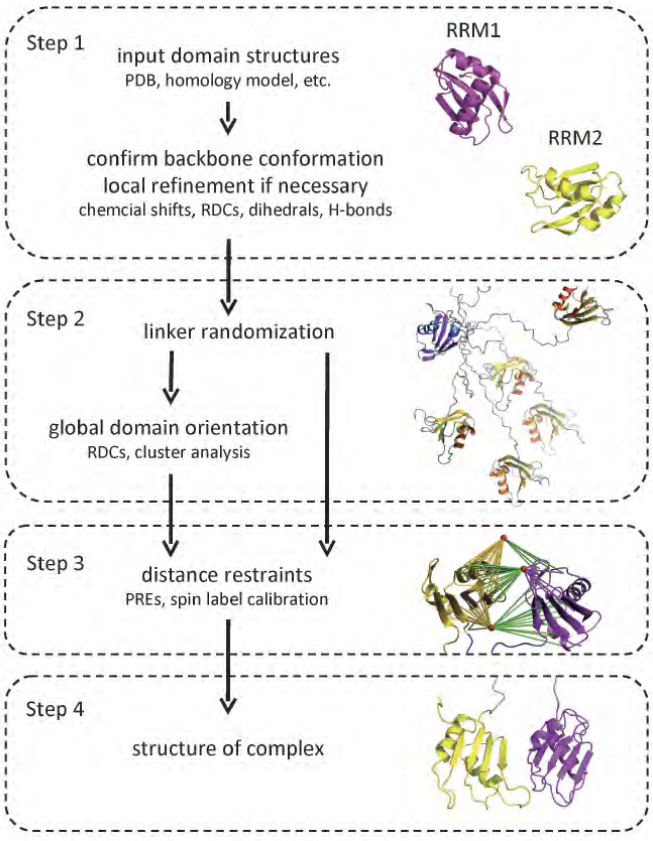

Domain arrangements from PRE data

- Individual domain structures available
- Spin labeling ⇔ paramagnetic relaxation enhancements (PRE)
- → distance restraints to define interdomain arrangement

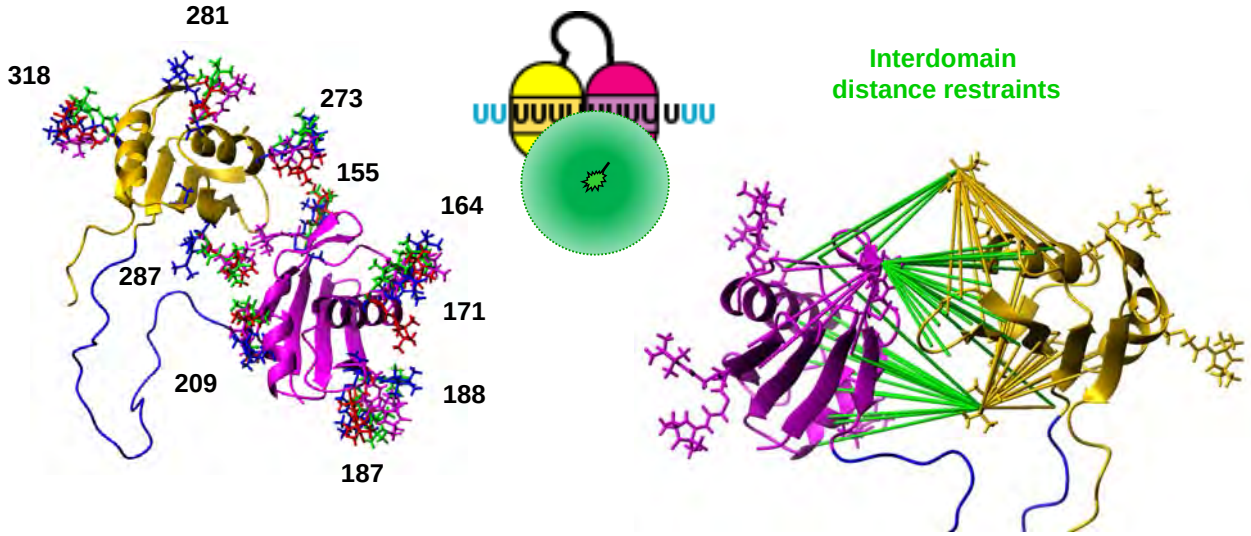

Simon, et al Angew. Chem. (2010); Madl et al JACS (2010) ; Mackereth et al Nature (2011)
Iwahara, Schwieters, Clore, JACS 126, 8579 (2004); Clore & Iwahara, Chem Rev (2009);

PRE data define the domain arrangements

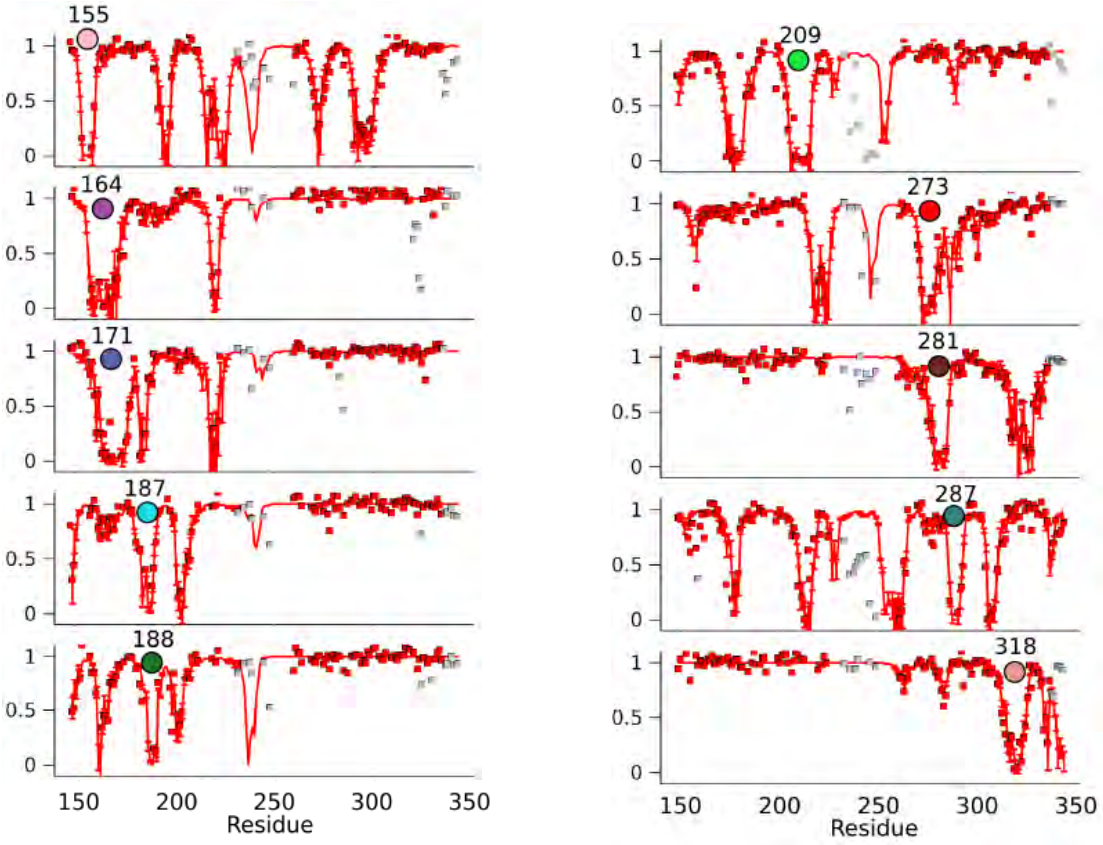

Open and closed conformations of U2AF65

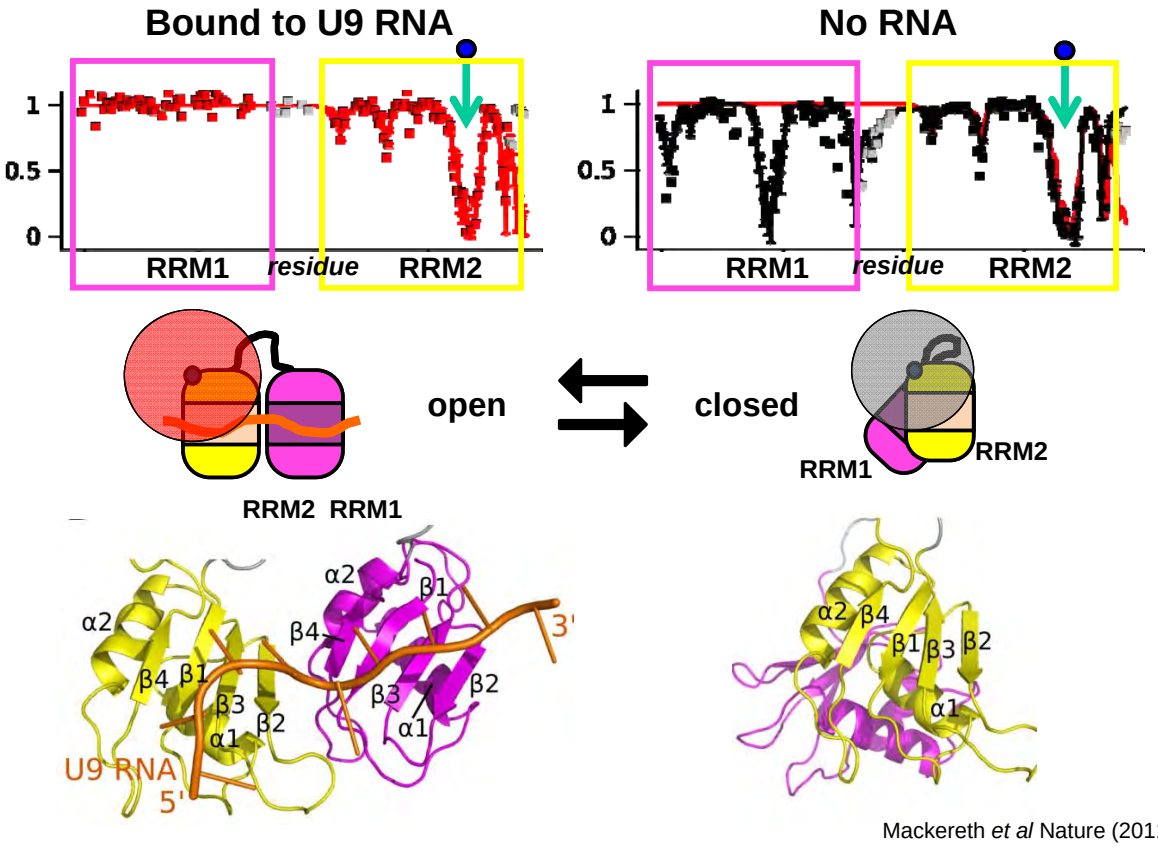

Mackereth *et al* Nature (2011)

Solution conformation differs from crystal structure

NMR

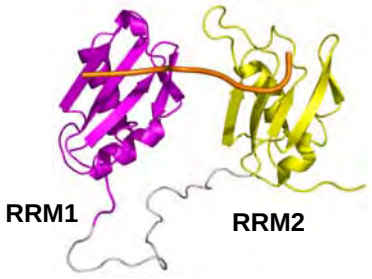

X-ray

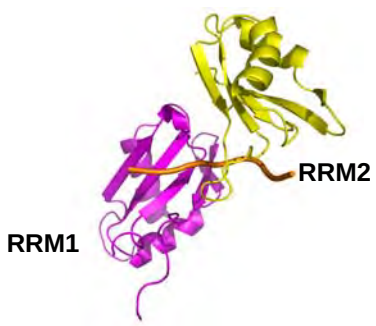

Importance of using solution methods for studying multidomain proteins

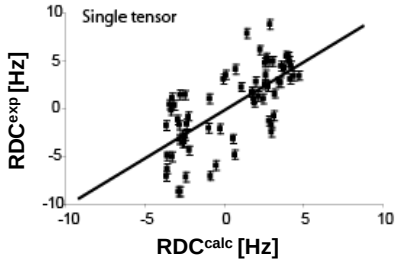

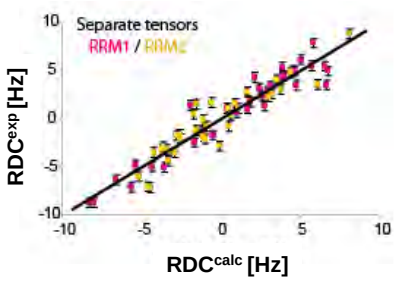

Sickmier et al *Mol. Cell* (2006)

Conformational shift measures Py tract "strength"

Human U2 introns

K_D /μM	
33	UUUU U4
18	UUUUAAAA U4A4
16	UUUUAAAAAAAAUUUU U4A8U4
7.1	UUUUAAAAUUUU U4A4U4
1.3	UUUUUUUUU U9
0.35	UUUUUUUUUUUUU U13

Py tract "strength"

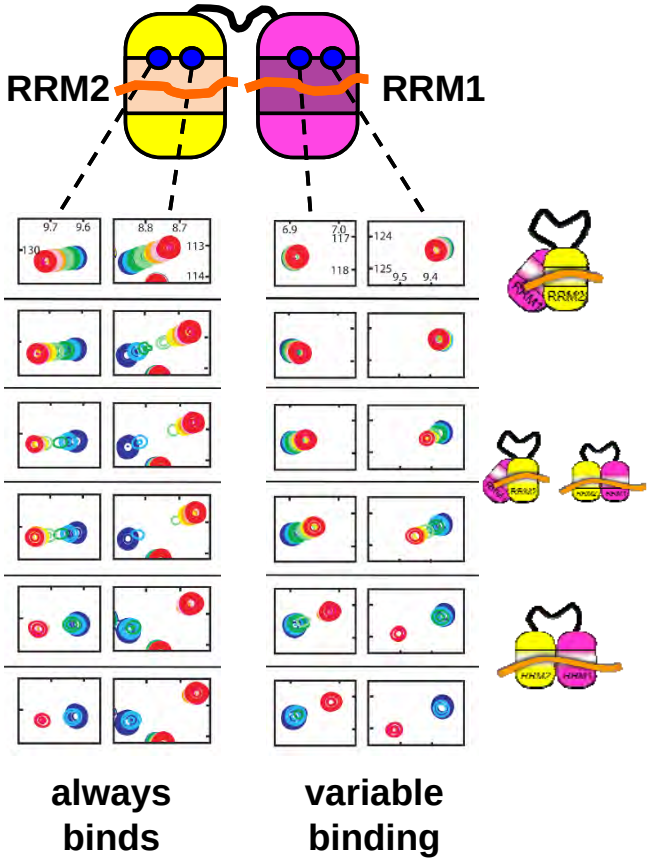

Population shift of distinct domain arrangements

Kd /μM	unbound
33	UUUU U4
18	UUUUAAAA U4A4
16	UUUUAAAAAAAAUUU U4A8U4
7.1	UUUUAAAAUUUU U4A4U4
1.3	UUUUUUUUU U9

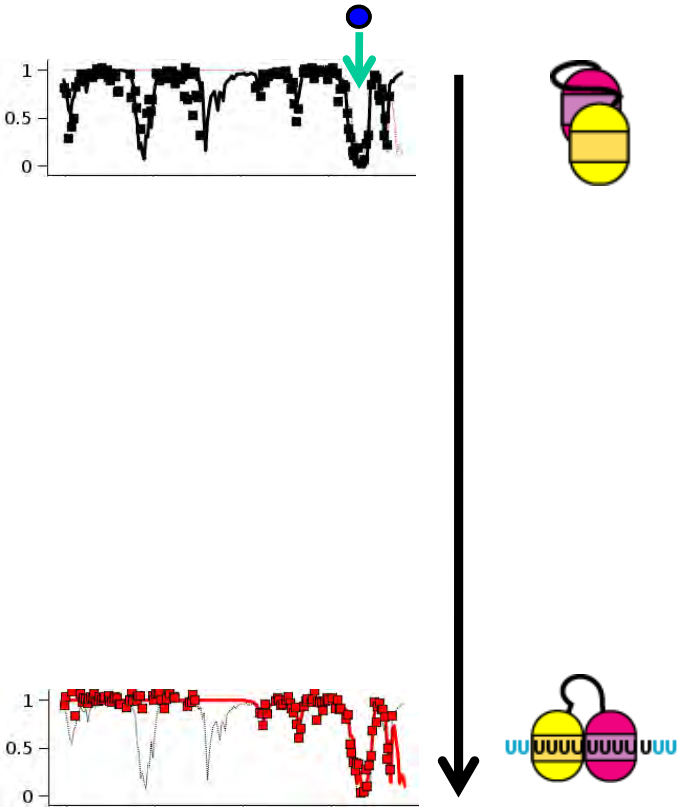

Pre-existing “bound” conformations in free RRM1-RRM2

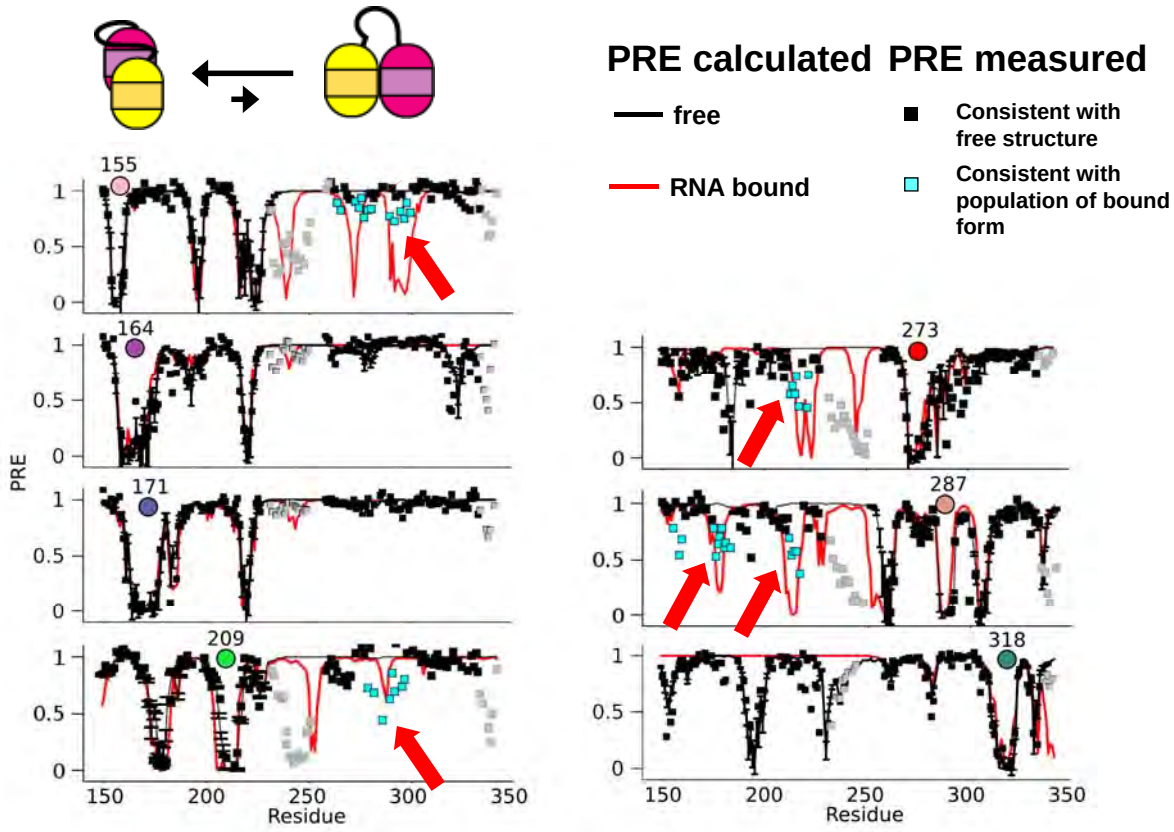

Free U2AF65 samples non-compact conformations

- Small Angle Scattering data indicate non-compact conformations in free RRM1,2

  → free RRM1,2 is an ensemble of compact and non-compact states
- In contrast, RRM1,2/RNA is compact

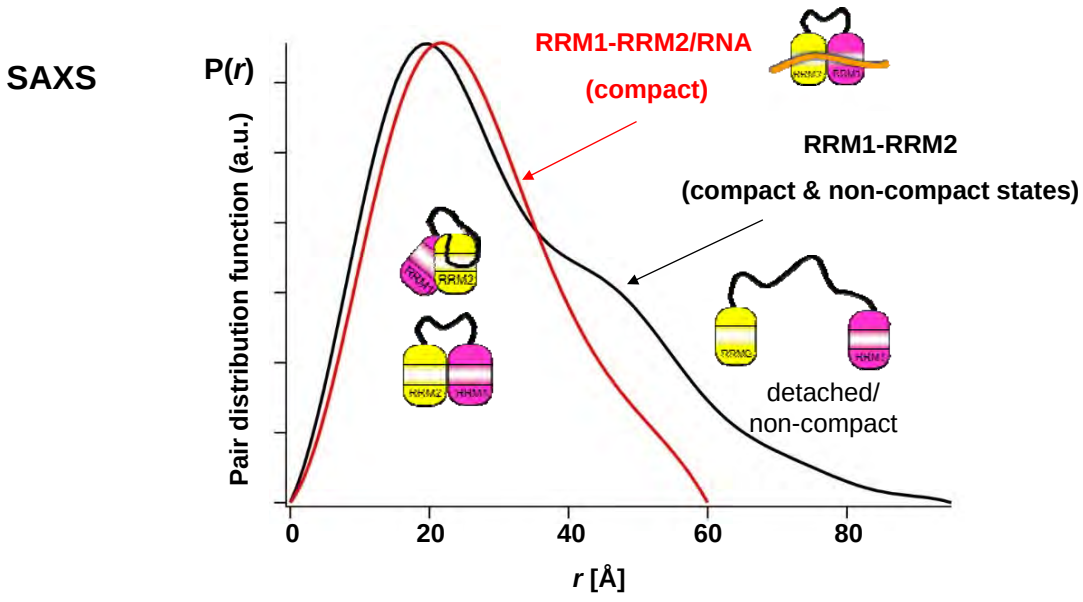

Ensemble of RRM1,2 based on NMR and SAS data

Ensemble with randomized linker

Unbiased/unrestrained selection of conformations and populations

Monte-Carlo based error analysis

Center-of-mass of RRM2:

full ensemble (pool)

selected

closed

open

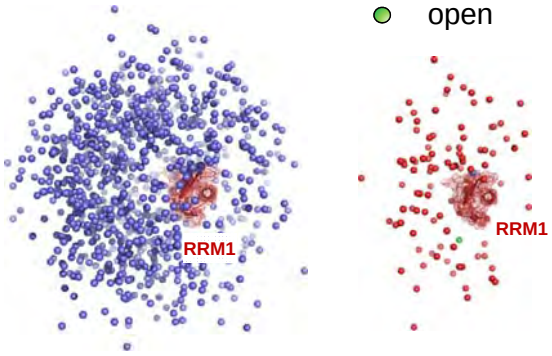

Jie-Rong Huang, Martin Blackledge

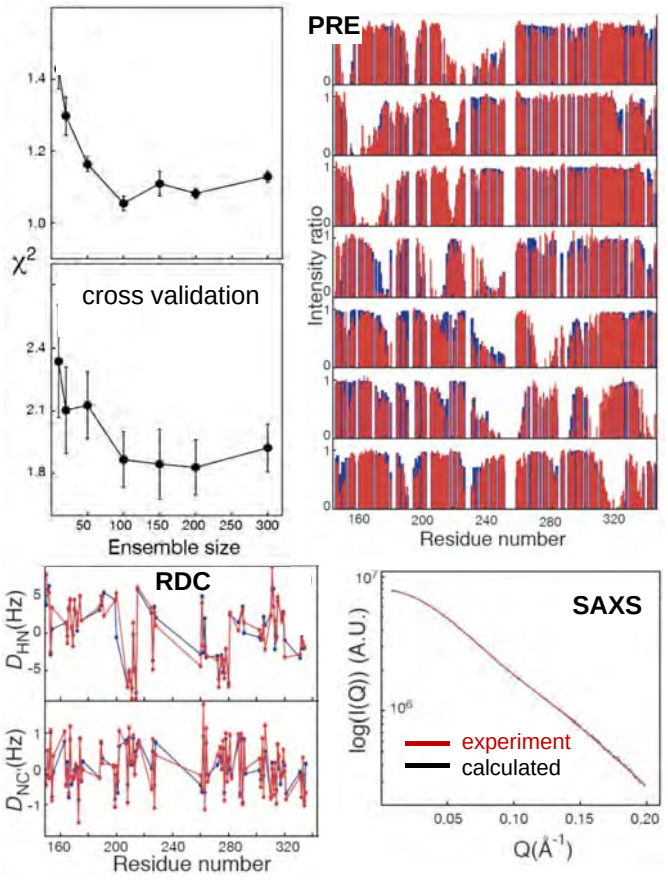

Ensemble of free states selected from NMR & SAXS

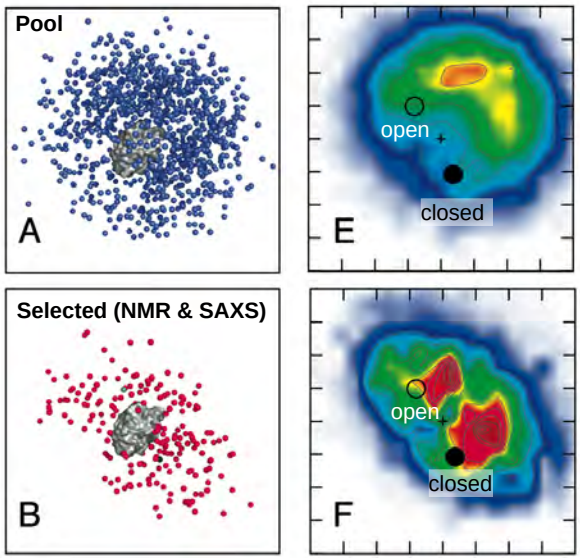

Enriched conformations (difference F-E)

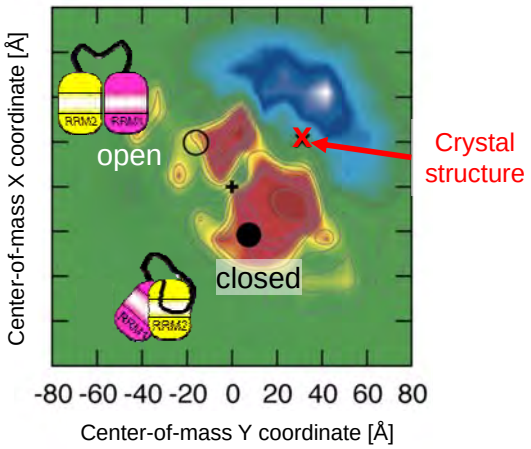

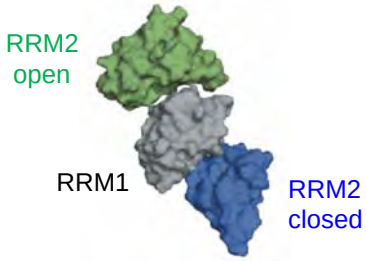

Huang et al, JACS (2014)

Ensemble of free states selected from NMR & SAXS

~50% of conformations are encounter-like, i.e. compact domain arrangement (consistent with ^{15}N NMR relaxation data)

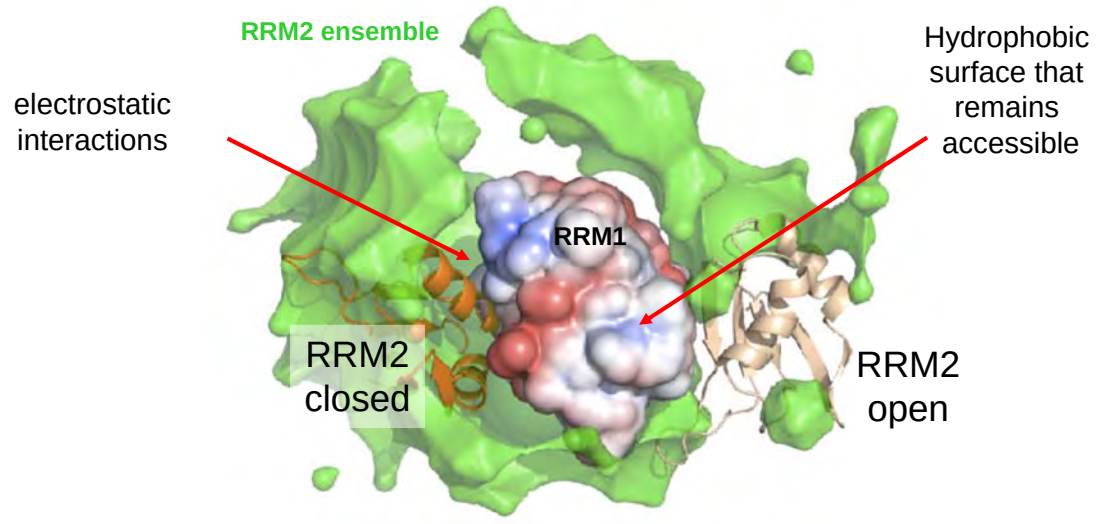

Huang et al, JACS (2014)

Modulation of encounter-like domain interactions

- PRE for spin-labeled A318C RRM1,2 at different salt concentrations
- Encounter-like charged interactions are salt dependent

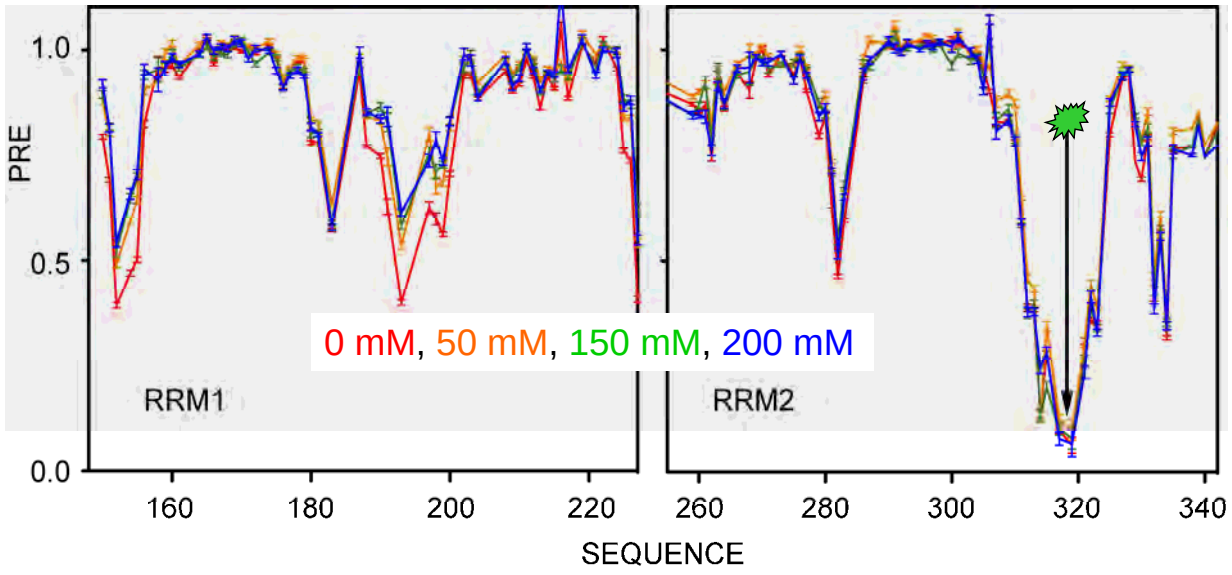

Complex mechanisms of RNA recognition in solution

Autoinhibition by linker → proof-reading

Dynamic ensemble of inactive states → conformational entropy

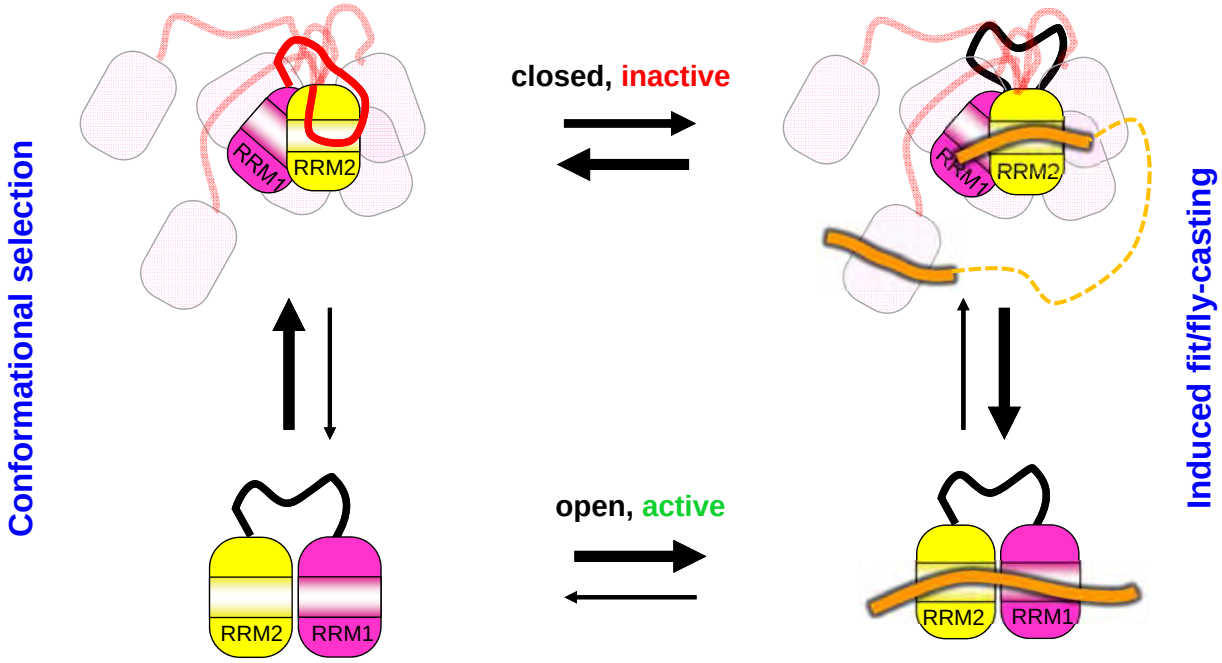

Key recognition elements in the ternary complex

Large induced fit of the RNA ligand and Sxl/CSD domain arrangement

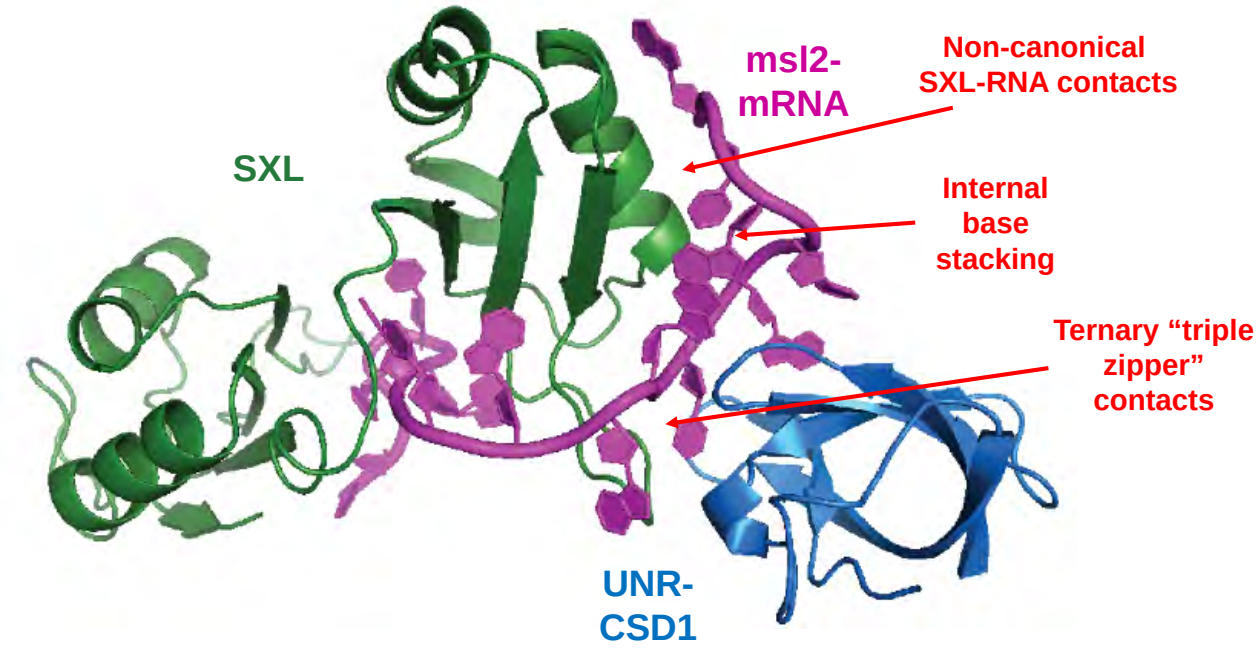

Hennig, et al, Nature (2014)

Structure validation in solution by NMR – UNR-CSD1

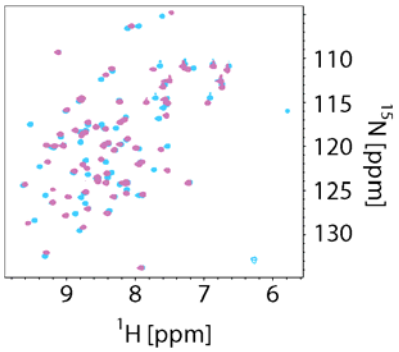

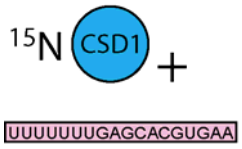

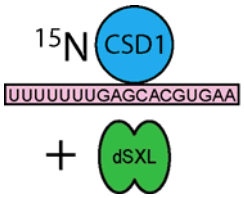

UNR-CSD1

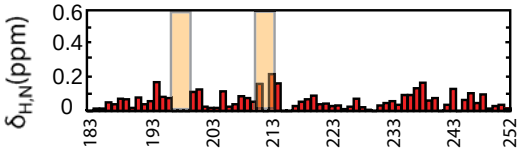

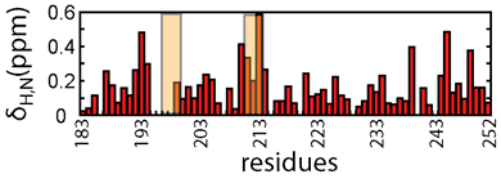

Ternary "triple zipper" contacts

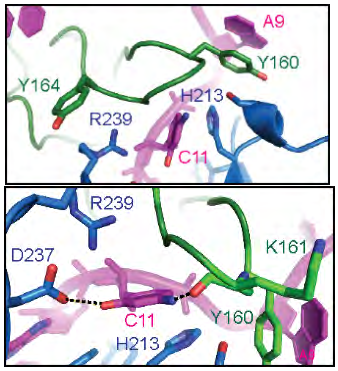

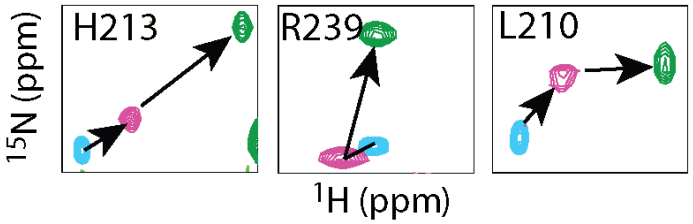

Triple zipper residues

Relative domain orientations in solution from NMR RDCs

RDC data in ternary complex agree with domain orientation in crystal structure

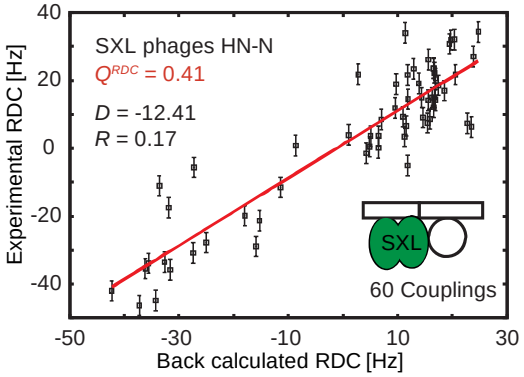

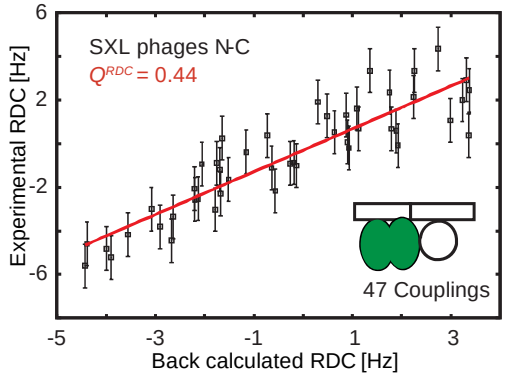

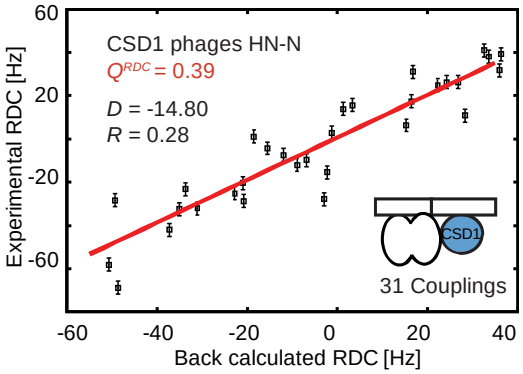

Joint NMR/X-ray refinement possible

(collaboration with Claudio Luchinat)

Structure validation in solution by SAXS and SANS

- SAXS and SANS data fully corroborate the crystal structure in solution
- MW I(0) = 34.2 kDa, expected: 33.5 kDa

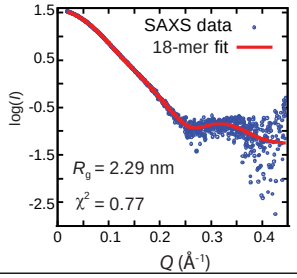

SAXS

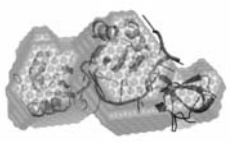

DAMMIN

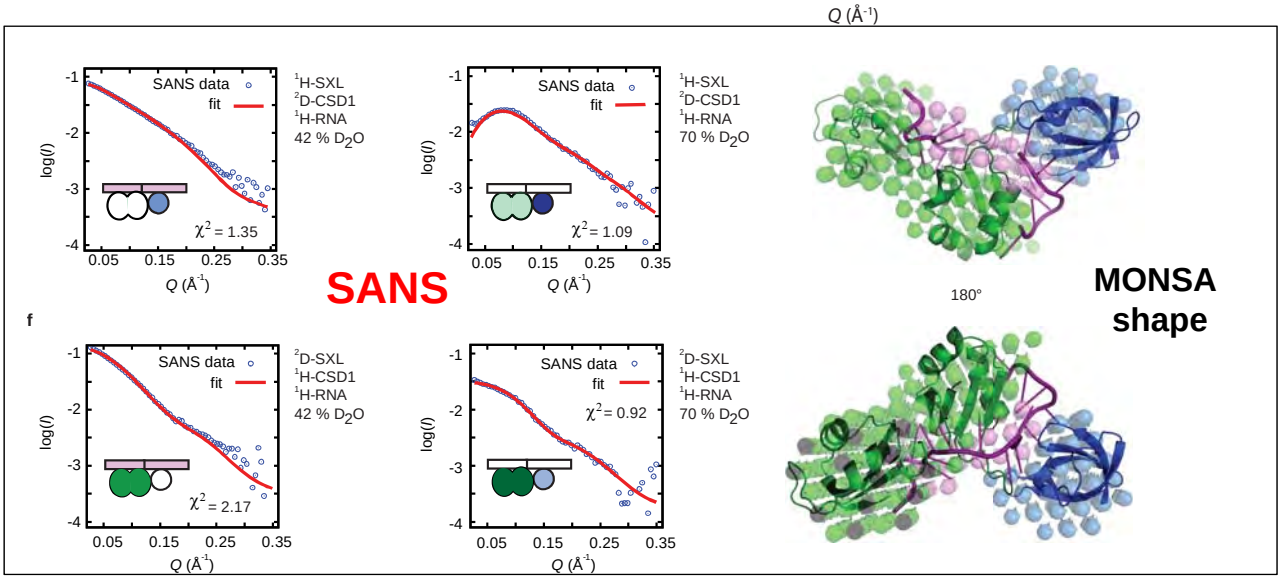

Summary

- Structure and dynamics of protein complexes in solution:
  - RDCs for relative domain arrangements
  - PREs/ spin-labeling for long-range distance restraints
  - PELDOR/DEER to measure specific distances and detect dynamics
    - Sensitive, no limitations by molecular weight, spin-labeling required
- Solvent PRE to detect and refine domain interfaces
  - Simple to measure, no protein modification required, dynamics affects analysis
- SAXS as complementary technique
  - Detect conformational equilibria/dynamics
  - Joint structural refinement
  - Need to combine with additional experimental data to reduce/resolve ambiguities

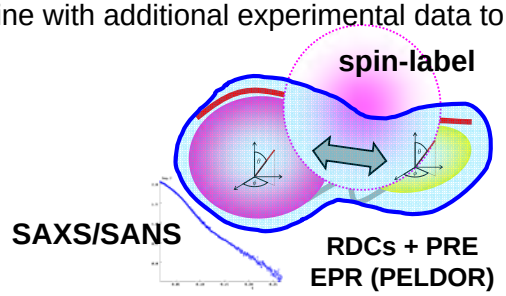

Conclusions

- Structural dynamics of multi-domain RNA binding proteins is important for their functional activity

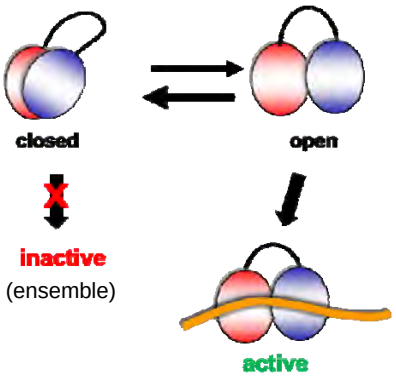

- Cooperative binding of multiple RNA binding domains (RBDs) expands the protein-RNA interaction network to regulate diverse biological functions with a limited set of RBDs: → protein-RNA recognition code

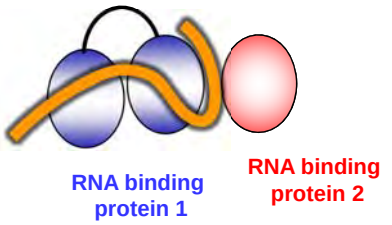

- Integrated structural biology –solution techniques, i.e. NMR, SAXS, SANS to study dynamics of multi-domain proteins and complexes

Funding